

Effect of Pavement Temperature on Frictional Properties of Hot-Mix-Asphalt Pavement Surfaces at the Virginia Smart Road

Yingjian Luo

Thesis Submitted to the Faculty of
Virginia Polytechnic Institute and State University
In partial fulfillment of the requirements for the degree of:

Master of Science
In
Civil and Environmental Engineering

Dr. Gerardo Flintsch, Chair
Dr. Imad L. Al-Qadi
Dr. Amara Loulizi

January 8, 2003
Blacksburg, Virginia

Keywords: Pavement Friction, Pavement Temperature, Pavement Surface Characteristics, Skid Number

©Copyright 2003, Yingjian Luo

Effect of Pavement Temperature on Frictional Properties of Hot-Mix-Asphalt Pavement Surfaces at the Virginia Smart Road

Yingjian Luo

Chair: Dr. Gerardo Flintsch

The Via Department of Civil and Environmental Engineering

Abstract

Wet-pavement friction is a public concern because of its direct relation to highway safety. Both short- and long-term seasonal variations have been observed in friction measurements. These variations have been attributed to different factors, such as traffic, rainfall, and temperature. Since both the tire rubber and the HMA pavement surface are viscoelastic materials, which are physically sensitive to temperature changes, temperature should affect the measured frictional properties. Although several researchers have attempted to explain and quantify the effect of temperature on pavement friction, it remains to be fully understood.

The objective of this research was to quantify the effect of pavement surface temperature on the frictional properties of the pavement-tire interface. To accomplish this, tests conducted on seven different wearing surfaces at the Virginia Smart Road under different climatic conditions were analyzed. Due to the short duration of this study and the low traffic at the facility, only short-term effects of temperature on pavement friction were investigated.

To accomplish the predefined objective, skid test data from both ribbed and smooth tires were collected over two and a half years (from January 2000 to August 2002) and then analyzed. Six sets of tests were conducted under different environmental conditions. The pavement and air temperatures during each test were obtained using

thermocouples located directly under the wearing course (38mm below the surface) and close to the pavement surface, respectively. Regression analyses were conducted to determine the effect of pavement temperature on the measured skid number at different speeds, as well as on friction model parameters.

The main conclusion of this investigation is that pavement temperature has a significant effect on pavement frictional measurements and on the sensitivity of the measurements to the test speed. Both the skid number at zero speed (SN_0) and the percent normalized gradient (PNG) tend to decrease with increased pavement temperature. This results in the pavement temperature effect on the measured skid number being dependent on the testing speed. For the standard wearing surface mixes studied, at low speed pavement friction tends to decrease with increased pavement temperature. At high speed, the effect is reverted and pavement friction tends to increase with increased pavement temperature. Temperature-dependent friction versus speed models were established for one of the mixes studied. These models can be used to define temperature correction factors.

Acknowledgements

The author expresses his most sincere gratitude to his advisor, Dr. Gerardo Flintsch, for his guidance and assistance in completing this research. Thanks are also extended to committee members Dr. Imad Al-Qadi and Dr. Amara Loulizi for giving helpful comments and providing support.

The author extends his heartfelt appreciation to his wife and his family for their support and encouragement during his study at Virginia Polytechnic Institute and State University.

Table of Contents

Abstract.....	ii
Acknowledgements	iv
Table of Contents	v
List of Figures.....	vii
List of Tables	viii
Chapter 1 Introduction.....	1
1.1 Background.....	1
1.2 Problem Statement.....	3
1.3 Objectives	3
1.4 Scope	4
Chapter 2 Literature Review	5
2.1 Introduction.....	5
2.2 Pavement Friction Measuring Technologies	5
2.3 Pavement Friction Models	8
2.3.1 The Penn State Model.....	8
2.3.2 The Rado Model	9
2.3.3 The International Friction Index (IFI).....	10
2.4 Short- and Long- Term Environmental Effects on Pavement Friction.....	11
2.5 Temperature Effects.....	13
2.5.1 Air Temperature.....	14
2.5.2 Tire Temperature	14
2.5.3 Pavement Temperature	16
2.6 Other Possible Influential Factors.....	17
2.7 Pavement-Tire Friction Theory.....	18
2.8 Summary	21
Chapter 3 Experimental Program.....	22
3.1 The Virginia Smart Road	22
3.2 Volumetric Properties of the Wearing Surface Mixes.....	23
3.3 Friction Tests	24
3.3.1 Locked Wheel Skid Trailer.....	25
3.3.2 Skid Number Computation	26
3.3.3 Calibration of Locked Wheel Skid Trailer.....	28
3.3.4 Testing Program.....	28

3.4 Pavement Temperature	29
3.4.1 Pavement Temperature Measurements	30
3.4.2 Pavement Temperature Verification Tests.....	31
Chapter 4 Data Collection and Analysis.....	32
4.1 Data Collection	32
4.1.1 Pavement Friction Measurements.....	32
4.1.2 Temperature Data.....	35
4.2 Data Analysis.....	37
4.2.1 Regression Analysis.....	37
4.2.1.1 SN_S Analysis	38
4.2.1.2 SN_R Analysis	40
4.2.1.3 Model Verification	42
4.2.2 Temperature Effect on SN_0 and PNG	43
4.2.2.1 Smooth Tire Measurements.....	44
4.2.2.2 Ribbed Tire Measurements	46
4.2.2.3 Model Verification	48
4.3 Effect of Water on Pavement Temperature	51
4.4 Summary and Discussion.....	52
Chapter 5 Findings and Conclusions	55
5.1 Findings.....	55
5.2 Conclusions.....	56
Chapter 6 Recommendations.....	57
References	58
Appendix A: Raw Skid Test Data	62
Appendix B: Pavement Surface Temperature Data	171
VITA	184

List of Figures

Figure 2.1 Locked Wheel Skid Trailer	7
Figure 2.2 Mechanistic Model for SN_0	11
Figure 2.3 Mechanism of Rubber Friction (Kummer and Meyer, 1962).....	19
Figure 3.1 Prewetting System of Skid Trailer	26
Figure 3.2 T-shape Thermocouple.....	29
Figure 4.1 Average Skid Numbers Measured Using the Smooth Tire (SN_S).....	33
Figure 4.2 Average Skid Numbers Measured Using the Ribbed Tire (SN_R).....	34
Figure 4.3 Pavement Temperature Profile for Section B in a Typical Day.....	36
Figure 4.4 SN_S versus Pavement Temperature for Sections E through H.....	38
Figure 4.5 SN_R versus Pavement Temperature for Sections E through H.....	40
Figure 4.6 Exponential Regression for the Section A Test Set 5B-IU	44
Figure 4.7 SN_{S0} and PNG versus Pavement Temperature for Sections E through H.....	45
Figure 4.8 SN_{R0} and PNG versus Pavement Temperature for Sections E through H.....	47
Figure 4.9 SN_S Friction Models for Sections E through H at 0, 25 and 50°C	49
Figure 4.10 SN_R Friction Models for Sections E through H at 0, 25 and 50°C	50
Figure 4.11 Skid Number versus Speed at Different Temperatures.....	53

List of Tables

Table 2.1 Reference List of Different Temperature Formats Used in Studies	15
Table 3.1 Wearing Surface Mixes Used at the Virginia Smart Road	23
Table 3.2 Properties of the HMA Wearing Surfaces	24
Table 3.3 SN Data for Ribbed Tire Uphill Direction on the Instrumented Lane of Section A.....	27
Table 3.4 Time Information of Skid Tests.....	28
Table 3.5 Example of Measured Pavement Temperature.....	30
Table 4.1 Example Output of the Temperature Monitoring System for Section B	35
Table 4.2 Average Pavement Temperature ($^{\circ}\text{C}$) 38 mm below Surface for All Tests.....	37
Table 4.3 SN_S Regression Analysis Results (Sections E through H)	39
Table 4.4 SN_S Regression Analysis Results for All Individual Sections.....	39
Table 4.5 SN_R Regression Analysis Results (Sections E through H)	41
Table 4.6 SN_R Regression Analysis for All Individual Section.....	41
Table 4.7 SN_S Regression Analysis Results Using Two Testing Dates (4B and 5B).....	42
Table 4.8 SN_R Regression Analysis Results Using Two Testing Dates (3T and 5T).....	43
Table 4.9 Calculated SN_{S0} and PNG (hr/km) for Sections E through H	45
Table 4.10 SN_{S0} and PNG (hr/km) Regression Analysis Results for All Sections.....	46
Table 4.11 Calculated SN_{R0} and PNG (hr/km) for Sections E through H	47
Table 4.12 Calculated SN_S for All Sections at 0, 25 and 50°C	48
Table 4.13 Calculated SN_R for All Sections at 0, 25 and 50°C	49
Table 4.14 Average Surface Temperature ($^{\circ}\text{C}$) Data of the Temperature Tests.....	51
Table 4.15 Paired T-test of Temperature Effect of Water on Pavement	52

Chapter 1

Introduction

1.1 Background

Wet pavement crashes are a significant problem and are a major concern of most highway agencies. The National Transportation Safety Board (NTSB, 1980) reported that in the United States, fatal crashes occur on wet pavements at a rate of from 3.9 to 4.5 times the rate of occurrence on dry pavements. Another nationwide study (FHWA, 1990) reported that of almost 25 million reported crashes, 18.8% occurred on wet pavements. One of the contributors to wet-pavement crashes is skidding. Skidding happens most frequently when the pavement surface does not provide adequate friction. Wambold et al. (1986) studied the relationship between wet-weather crashes and sites with low skid numbers, which were measured using a skid trailer (ASTM E-274). No statistically significant correlation was found between the skid numbers measured using a ribbed tire (ASTM E-501) and wet-weather crashes. On the contrary, the skid numbers measured with smooth tire (ASTM E-524) showed a significant correlation with wet-weather crashes (Wambold, 1986). As a result, smooth test tires are used as predictor of skid crash potential.

Skid resistance is monitored using different types of skid testing devices. The locked-wheel trailer is the most commonly used device in the United States. Skid tests are subject to many influential factors, which can be generally classified into three categories (Henry, 1986): tire-related factors (rubber compound, tread design and condition, inflation pressure, and operating temperature); pavement-related factors (pavement type, microtexture and macrotexture, and surface temperature); and intervening-substance-related factors (quantity of water, presence of loose particulate matter, and oil contaminants). While the testing is conducted in wet conditions, the water film covering the pavement acts as a lubricant and reduces the contact between the tires and the surface aggregate (Jayawickrama and Thomas, 1997). This is one of the reasons

why wet-pavement surfaces exhibit lower friction than dry pavement surfaces. In addition to the lubricating effects of water, at high speed, certain depths of water film may result in hydroplaning (Agrawal and Henry, 1979).

Conventional friction theories agree that friction at the tire-pavement interface has two principal components: adhesion and hysteresis (Bowden and Tabor, 1950). Adhesive shear forces are generated when the tire rubber slides over the aggregate surface asperities (microtexture) and the aggregate particles penetrate the rubber. The hysteresis component of the friction is developed when the tire rubber deforms because of the irregularities of the pavement surface (macrotexture). Therefore, the frictional properties of the pavement surface depend on both the surface microtexture and macrotexture (ASTM E-867). These properties are conditioned by several material design and construction properties, including aggregate type and gradation, degree of compaction in asphalt pavements, and texturing method in concrete pavements.

Traffic and weather-related factors also affect the surface microtexture and macrotexture properties of in-service pavements, and thus the pavement friction. Traffic wears the pavement surface and polishes the aggregate. Its effect is cumulative with time. Weather-related factors, such as rainfall, air temperature, wind, and dry days before the test day, are partially responsible for short-term and long-term variation in the frictional properties of the tire-pavement interface. For example, air temperature determines the pavement surface temperature and it has a short-term effect. Similarly, rainfall produces short-term variations. Skid numbers typically decrease and reach a minimum value after seven days of dry weather (Hill and Henry, 1978). These environmental effects combine to produce seasonal variations in the pavement frictional properties. Seasonal variations of pavement surface friction were first reported in Virginia by Giles and Sabey (1959). Although a number of models have been established to depict the effects of seasonal variation, some of the mechanisms and relevant factors are still not completely understood. The effect of pavement surface temperature on friction is one such factor.

A number of researchers have investigated the effect of temperature on pavement frictional properties. One of the problems encountered while reviewing these efforts is that the type of temperature used in these studies has not been consistent. For example, Runkle and Mahone (1980) considered the maximum, minimum and average daily temperatures; Burchett and Rizenbergs (1980) considered the maximum and minimum air temperature during a four to eight - week period; and the National Safety Council (1975) used the pavement surface temperature to correlate with pavement friction. Furthermore, the investigations conducted so far have not produced consistent results. While some researchers (Runkle and Mahone, 1980; Burchett and Rizenbergs, 1980) indicated a statistically significant effect of air or pavement temperature on the skid properties, others (Mitchell et al., 1986) concluded that the effect was insignificant.

1.2 Problem Statement

Environmental factors, such as temperature, rainfall, and dry days before the test day, are believed to cause seasonal variations in the frictional properties of pavements. However, there is no clear understanding of how these factors relate with observed short- and long-term pavement friction fluctuations. Although several researchers have attempted to explain and quantify the effect of temperature on pavement friction, this effect remains to be completely understood.

1.3 Objectives

The objective of this thesis is to quantify the effect of pavement surface temperature on the frictional properties of the pavement-tire interface. To accomplish this, tests conducted on seven different wearing surfaces at the Virginia Smart Road under different climatic conditions were analyzed; short- and long- term effects of temperature on pavement friction were investigated. However, due to the short duration of this study and the low traffic on the facility, the long-term effect was not considered. The study focused on pavement surface temperature effect.

1.4 Scope

To accomplish the predefined objective, skid test data collected over two and a half years (from January 2000 to August 2002) using both ribbed and smooth tires were analyzed. Six sets of tests were conducted under different environmental conditions. The pavement and air temperature during each test were obtained using thermocouples located directly under the wearing course (38mm below the surface) and close to the pavement surface, respectively. Regression analyses were conducted to determine the effect of pavement temperature on the measured skid number at different speeds, as well as on friction model parameters.

In this thesis, Chapter 2 contains a review of literature pertaining to fundamental friction theories and models, factors affecting pavement friction, and seasonal variations of pavement friction. Chapter 3 presents the experimental program conducted and discusses the pavement surfaces studied, the friction-measuring equipment utilized, and the temperature data collected. Chapter 4 summarizes the data collected, the analysis performed, and the results obtained from this research. Chapter 5 presents the most relevant findings and conclusions, and Chapter 6 outlines recommendations for future research.

Chapter 2

Literature Review

This chapter discusses the main literature related with pavement friction measurement and the effect of temperature on these measurements. Basic concepts, testing devices, testing standards, fundamental friction theories, and friction models are discussed. Seasonal pavement friction variations, influencing factors and, especially, temperature effects are emphasized.

2.1 Introduction

The safety of a pavement surface is primarily related to the surface friction, or skid resistance, and surface texture of the pavement. Each year there are between 45,000 and 50,000 accidental fatalities in the U.S., and approximately 15 percent of accidents that result in an injury or a fatality occur during wet weather conditions (Smith, 1975). In addition to the loss of human lives, the cost of property damage, traffic delays, and operations is very high. A recent study by the National Highway Traffic Safety Administration (NHTSA) showed that the economic impact of motor vehicle crashes on America's roadways has reached \$230.6 billion per year, or an average of \$820 for every person living in the United States (NHTSA, 2002). These accidents result from numerous reasons such as driver error, vehicle malfunction, and friction deficiencies at the tire-pavement interface.

2.2 Pavement Friction Measuring Technologies

There are four basic types of full-scale, high-speed friction measuring devices: locked wheel, side force, fixed slip, and variable slip. Some of the systems detect the peak friction and some vary the slip in an attempt to operate around the peak friction level (Henry, 2000). The values produced by the different devices relate to different scenarios. The locked wheel method simulates emergency braking without anti-lock

brakes, the side force method measures the ability to maintain control in curves, and the fixed slip and variable slip methods relate to braking with anti-lock brakes. Most U.S. agencies use locked wheel skid trailers (ASTM E-274).

The locked wheel friction measuring devices provide a coefficient of friction for a standard set of test conditions, which is typically reported as a skid or friction number (Burchett and Rizenbergs, 1980). The device locks one of the wheels, measures the vertical and horizontal forces on the test tire, and computes the skid number using equation 2.1.

$$SN_v = F / N * 100 \quad (2.1)$$

where

F = friction force;

N = normal (vertical) load on the test tire; and

V = test speed.

Typical devices used worldwide include the Skid Resistance Trailer (USA), Stuttgarter Reinsungsmesser SRM (Germany), LPC (France), Skiddometer BV8 (Switzerland), Corbirt Trailer (Portland), and Kotuki (PIARC Hungary). A computerized locked wheel Skid Trailer was used for this investigation at the Virginia Smart Road. The locked wheel skid trailer (Figure 2.1) has the following advantages: it is accurate, testing is conducted quickly and safely, and the equipment is easily transported (towed by a regular pick-up truck). On the other hand, one disadvantage of locked wheel devices is that they do not provide a continuous measurement. When the test wheel is intermittently locked for measurement, low friction areas may be overlooked. The locked wheel trailer also presents problems when measuring skid resistance at curves (Burchett and Rizenbergs, 1980).

Side force systems maintain the test wheel in a plane at an angle (the yaw angle) to the direction of motion; otherwise, the wheel is allowed to roll freely. The side force (cornering force) is measured perpendicular to the plane of rotation. An advantage of this method (Henry, 2000) is that these devices can measure continuously through the test

section. A popular disadvantage of the side force system is the cornering speed could be very low by multiplying the driving speed with yaw angle. Typical side force devices are the Mu Meter and the Side-force Coefficient Road Inventory Machine (SCRIM).



Figure 2.1 Locked Wheel Skid Trailer.

Fixed slip devices operate at a constant slip, usually between 10 to 20 percent. The test wheel is driven at a lower angular velocity than its free rolling velocity. This is accomplished by incorporating a gear reduction or chain drive or by hydraulic retardation of the test wheel. These devices measure low-speed friction, as the slip speed is the vehicle speed multiplied by the percent slip. Like the side force method, the fixed slip method can be operated continuously over the test section without excessive wear of the test tire.

Variable slip devices sweep through a predetermined set of slip ratios using a hydraulic motor that actuates over the test wheel. ASTM Standard E-1859 has been developed for devices that perform a controlled sweep through a range of slip ratios.

In addition to the high-speed devices presented, portable devices, such as the British Pendulum Tester and the Dynamic Friction Tester (DFTester), can be used to test both laboratory cores and actual pavements. The results of BPT and DFtester are affected mainly by the microtexture of the pavement surface.

2.3 Pavement Friction Models

Since pavement friction is highly dependent on the testing speed, in order to depict the complete frictional properties of a pavement surface, it is necessary to either conduct tests using at least two different speeds, or to measure other surface properties, such as macrotexture. Three primary models have been proposed to depict the relation between friction and speed: the Penn State Model, the Rado Model, and the International Friction Index (IFI) Model, which is basically an extension of the Penn State Model. The most frequently used model is the Penn State/IFI model, according to which the SN decreases exponentially with speed.

2.3.1 The Penn State Model

One of the first skid models was proposed at the Pennsylvania State University (Leu and Henry, 1976) and is known as the Penn State Model. This model describes the relationship of friction (μ) to speed (S) using the exponential function presented in Equation 2.2.

$$\mu = \mu_0 e^{-\frac{PNG \cdot S}{100}} \quad (2.2)$$

where

μ_0 = intercept of friction at zero speed; and

PNG = percent normalized gradient, defined by Equation 2.3.

$$PNG = -\frac{100}{\mu} \frac{d\mu}{ds} \quad (2.3)$$

Researchers agree that PNG is highly correlated with macrotexture and that μ_0 can be predicted mostly from microtexture (Henry, 2000). Later versions of the Penn State Model replaced the term [PNG/100] by a speed constant S_p , resulting in Equation 2.4.

$$\mu = \mu_0 e^{-\frac{S}{S_p}} \quad (2.4)$$

This replacement of PNG by Sp (speed constant) can be attributed to the following reasons (Kulakaowski, 1993):

1. The defined PNG is actually the opposite of the normalized gradient of friction versus speed. The negative sign in Equation 2 may be misleading since positive PNG values may erroneously suggest that pavement friction increases with speed.
2. Multiplying the normalized gradient by 100 does not quite justify the use of the word “percent” in PNG. The word “percent” implies that a PNG equal to 100 percent has special and clear significance, but it has none. Furthermore, it is totally unrealistic; PNG values for existing pavements seldom exceed 3 to 4 percent.
3. The use of the term “percent” is inappropriate because the physical units of PNG are hour per mile or hours per kilometer and not percent.

The IFI Model that is discussed in Section 2.3.3 adopted the modified Penn State Model, but shifted the intercept to 60 km/h (ASTM E-1960-98), resulting in Equation 2.5.

$$F(S) = F60e^{\frac{60-S}{S_P}} \quad (2.5)$$

where

F(S) is the friction at slip speed S, and
F60 is the friction at 60 km/h (36 mph).

2.3.2 The Rado Model

As a tire proceeds from the free rolling condition to the locked wheel condition under braking, the friction increases from zero to a peak value and then decreases to the locked wheel friction. Anti-lock brake systems release the brakes to attempt to operate around the peak level of friction. The Rado Model depicts the entire braking maneuver using the following equation (Henry, 1986):

$$\mu(S) = \mu_{peak} e^{-\left[\frac{\ln(S/S_{peak})}{C}\right]^2} \quad (2.6)$$

where

μ_{peak} = peak friction level,

S_{peak} = slip speed at the peak (typically 15% of the vehicle speed), and

C = shape factor related to the harshness of the texture.

The Penn State and Rado Models together can be used to simulate the complete vehicle braking in an emergency situation. The Rado Model is used at the beginning of the braking maneuver until the peak value is reached; after that the Penn State Model is more appropriate.

2.3.3 The International Friction Index (IFI)

The IFI consists of two numbers that describe the skid resistance of a pavement: the speed constant (S_p) and the friction number (F60). Measurement of both friction and macrotexture are needed to compute IFI. The speed constant is a linear function of the macrotexture measurement used (Equation 2.7).

$$S_p = a + bTX \quad (2.7)$$

where

TX = measured macrotexture value, and

a and b = regression coefficients for equations determined for the macrotexture measurement devices used in the PIARC experiment (ASTM E-1960).

The friction number (F60) is determined from a measurement of friction using Equation 2.8:

$$F60 = A + B * FRSe^{\frac{S-60}{S_p}} + C * TX \quad (2.8)$$

where

FRS = measurement of friction by a device operating at a slip speed (S), and

A, B, and C = regression coefficients of all variables for the friction measurement device used in the PIARC experiment (ASTM E-1960). The value of C is zero if the test uses a smooth tire, but the term C*TX is necessary for ribbed and pattern tires because these tires are less sensitive to macrotexture (Henry and Wambold, 1996).

2.4 Short- and Long- Term Environmental Effects on Pavement Friction

Pavement friction measurements experience temporal variations due to changes in pavement surface microtexture and macrotexture, as well as environmental conditions during testing. Both temperature and rainfall appear to affect the friction measurements. In most areas of America between north latitude 20 and 60, the monthly average temperature experiences a sinusoidal variation (NCDC, 1998). Hill and Henry (1982) proposed a mechanistic model to predict seasonal variations in skid number intercept (SN_0) based on the analysis of friction and climatic data collected on experimental test sites in Pennsylvania from 1978 to 1980. This model is presented in Equation 2.9 and is represented graphically in Figure 2.2.

$$SN_0 = SN_{0R} + SN_{0L} + SN_{0F} \quad (2.9)$$

where

SN_{0R} = short-term weather-related component of the skid number intercept;

SN_{0L} = long-term seasonal variation; and

SN_{0F} = a measure of SN_0 which is independent of both short- and long-term variations.

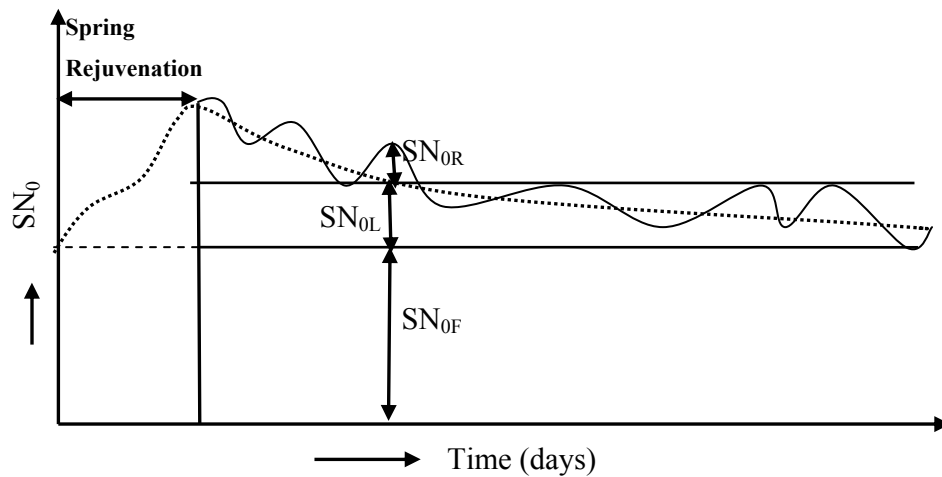


Figure 2.2 Mechanistic Model for SN_0

The long-term variations were found to follow an exponential relationship for asphalt surfaces as depicted in Equation 2.10.

$$SN_{OL} = \Delta SN_0 e^{-t/\tau} \quad (2.10)$$

where

ΔSN_0 = change in SN_0 over the testing season (year);

τ = rate at which long-term effects occur in asphalt surfaces; and

t = days from the beginning of tests.

The parameters ΔSN_0 and τ were found to depend on traffic (ADT) and the microtexture properties of the surface as indicated by Equations 2.11 and 2.12 (Hill and Henry, 1982).

$$\Delta SN_0 = 28.5 - 0.0023 \text{ ADT} - 0.09\text{BPN} \quad (R^2 = 0.67) \quad (2.11)$$

$$\tau = 67.67 - 0.0037 \text{ ADT} \quad (R^2 = 0.28) \quad (2.12)$$

where

BPN = British Pendulum Number; and

ADT = average daily traffic.

The short-term variation was found to be dependent on environmental factors, such as pavement temperature and dry days. The best-fit regression equation obtained in the study is presented in Equation 2.13. It must be noted that the correlation is very weak.

$$SN_{OR} = 3.79 - 1.17 \text{ DSF} - 0.104 T_P \quad (R^2 = 0.12) \quad (2.13)$$

where

DSF = dry spell factor = $\ln(t_R + 1)$;

t_R = number of days since the last rainfall of 2.5mm or more, $0 \leq t_R \leq 7$; and

T_P = pavement temperature ($^{\circ}\text{C}$).

Once the short- and long-term variations in SN_0 have been identified, these parameters can be used to correct the SN at 64km/hr (40 mph) as follows:

$$SN_{64F} = SN_{64} - (SN_{OR} + SN_{OL})e^{-0.64PNG} \quad (2.14)$$

where

SN_{64F} = SN at 64km/hr (40 mph) after removal of the short- and long-term effects; and
PNG = percent normalized gradient.

Although the model provides a comprehensive approach for analyzing seasonal variations, it also has serious deficiencies. Namely, the coefficient of determination in all the models is very low, the value of ΔSN_0 may change year after year, and although SN_{0F} is defined as independent of short- and long-term variation, it is in fact dependent on BPN and traffic.

2.5 Temperature Effects

Most studies agree that temperatures of the four elements interacting at the tire-pavement interface (air, water, tire, and pavement) affect pavement friction. Several investigations have studied these relationships; the most significant are reviewed in the following paragraphs. Although these studies have different temperatures and formats, researchers agree that these are highly correlated. For example, Runkle and Mahone (1980) found that water temperature and pavement temperature were highly correlated. Hill and Henry (1978) studied the relations between air temperature, pavement temperature, and tire temperature and concluded that the three temperatures are also highly correlated, as shown by Equations 2.15 through 2.17.

$$T_t = 8.54 + 0.810T_A \quad (R^2 = 0.83) \quad (2.15)$$

$$T_t = 6.78 + 0.558T_p \quad (R^2 = 0.76) \quad (2.16)$$

$$T_A = 0.87 + 0.573T_p \quad (R^2 = 0.80) \quad (2.17)$$

where

T_t = tire temperature ($^{\circ}C$),

T_p = pavement temperature ($^{\circ}C$), and

T_A = ambient temperature ($^{\circ}C$).

Table 2.1 summarizes the main studies that have evaluated the effect of temperature on pavement frictional properties. The table includes the reference cited,

location of the study, type of friction measurement studied, and the main effect observed. The most significant of these studies are discussed in detail in the following sections, organized by the type of temperature considered in the study.

2.5.1 Air Temperature

Many researches have studied the effect of air temperature on short-term variation in pavement friction. However, the type of temperature used has varied. While in some cases the temperature during testing was used, in other the temperature was averaged along periods of time that range from one day (Tung et al., 1977) to up to eight weeks (Burchett and Rizenbergs, 1980). Significant effects of air temperature were found in Texas (Jayawickrama and Thomas, 1997), Virginia (Runkle and Mahone, 1980), New York and Pennsylvania (Anderson et al., 1984). None of the reviewed references studied the effect of water temperature on the measured friction. The study conducted in Virginia (Runkle and Mahone, 1980) recorded water temperature, but this information was not used in the analysis.

Jayawickrama and Thomas (1997) observed that SN_{40} tends to decrease at high air temperature; they suggested that the temperature changes do not have a direct effect on the skid resistance, but rather change the frictional properties of tire rubber. Conversely, Mitchell et al. (1986) found the effect of temperature on skid resistance to be insignificant.

2.5.2 Tire Temperature

Kummer and Meyer (1962) found that the friction measured with British Pendulum Tester decrease at higher temperatures. The decrease in the friction coefficient could be due to an increase in the rubber temperature. This trend agrees with the results obtained in other studies.

Table 2.1 Reference List of Different Temperature Formats Used in Studies

Source	Study Locations	Type of Temperature ⁽¹⁾	Friction Parameter	Effect of Temperature on Friction
Kummer and Meyer (1962)	Florida	Slider Rubber Temperature	Friction Coefficient	Coefficient decreases with temperature
Tung et al. (1977)	Pennsylvania	T _p and average and maximum T _a (day and night time)	SN ₀	SN ₀ decreases with temperature
Hill and Henry (1978)	Pennsylvania	T _p	SN _{0R} (short-term SN ₀)	SN _{0R} decreases with temperature
Dahir et al. (1979)	Pennsylvania	T _p	SN ₀	SN ₀ decreases with temperature
Burchett and Rizenbergs (1980)	Kentucky	Average T _a during 4 to 8 weeks before the test	SN ₄₀	SN ₄₀ decreases with temperature
Runkle and Mahone (1980)	Virginia	Maximum, minimum, and average T _a on the test day or in one week before test	SN ₄₀	SN ₄₀ decreases with temperature
Elkin et al. (1980)	Indiana	T _p	SN ₄₀	SN ₄₀ decreases with temperature
Anderson et al. (1984)	New York, Virginia and Pennsylvania	T _a during testing	SN ₄₀	Significant temperature effect
Mitchell et al. (1986)	Maryland	T _a during testing	SN ₄₀	No significant effect observed
Oliver (1989)	Australia	T _p and T _t	SFC & SRV ⁽²⁾	SFC & SRV decrease with temperature
Jayawickrama and Thomas (1997)	Texas	T _a during testing (24 hr / 5 days)	SN ₄₀	SN ₄₀ decreases with temperature

⁽¹⁾ T_a = air temperature; T_p = pavement surface temperature; and T_t = tire temperature.

⁽²⁾ SFC = Side Force Coefficient; and SRV = Skid Resistance Value.

Oliver (1989) investigated in Australia the effect of tire temperature and found that cornering friction decreased with temperature according to Equation 2.18. This investigation also showed that the tire temperature is proportional to the air and pavement temperatures (Equation 2.19).

$$SFC_t / SFC_{25} = 0.563 + 45.9 / (t+80) \quad (R^2=0.83) \quad (2.18)$$

$$t = 12.3 + 0.48 * (T_a + T_p) \quad (2.19)$$

where

SFC_t = side force coefficient of SCRIM at tire temperature t ,

t = tire temperature ($^{\circ}C$),

T_a = air temperature ($^{\circ}C$), and

T_p = pavement temperature ($^{\circ}C$).

Hosking and Woodford (1976) have established similar equations between tire temperature and pavement friction which were used by the Transportation Road Research Laboratory (TRRL) in the United Kingdom.

Jayawickrama and Thomas (1997) hypothesized that temperature changes affect the properties of the rubber tire used in locked-wheel skid trailer tests because it affects the hysteresis component of the friction force. Hysteresis is the energy lost in the form of heat upon elastic recovery of the rubber tire, which is compressed as it slides over pavement. At higher temperatures the rubber becomes more flexible, leading to less energy loss. Higher temperatures thus lead to a decrease in the measured pavement surface friction.

2.5.3 Pavement Temperature

The investigation of the effect of pavement temperature on skid resistance has produced mixed results. Dahir et al. (1979) found that the short-term component of the skid number measurements SN_{OR} decreases with increased temperature (Equation 2.20).

Elkin et al. (1980) also found the same trend on the test using a locked wheel skid trailer conducted in Indiana.

$$SN_{OR} = 5.09 - 0.232T_p \quad (R^2=0.25) \quad (2.20)$$

where

T_p = surface pavement temperature ($^{\circ}\text{C}$).

Oliver (1989) also studied the seasonal variation of pavement friction in Australia using a British Pendulum Tester (BPT). This research project used a set of laboratory-prepared surfaces resembling normal pavement surfaces, which covered a range of skid resistance values between 15 and 90 units, and a range of surface textures between 0 and 1.5 mm. These prepared surfaces were tested outdoors with temperatures ranging from 7 to 59 $^{\circ}\text{C}$. This study observed a good correlation between the skid resistance value (SRV) measured with the BPT and pavement temperature (Equation 2.21). The researchers suggested that temperature (air and pavement temperature) determines the rubber temperature, which affects the viscoelastic properties of rubber.

$$SRV_t / SRV_{20} = 1 - 0.00525*(t-20) \quad (2.21)$$

where

t = prepared pavement surface temperature ($^{\circ}\text{C}$),

SRV_t = the skid resistance value obtained at temperature t ($^{\circ}\text{C}$), and

SRV_{20} = the skid resistance value obtained at 20 $^{\circ}\text{C}$.

2.6 Other Possible Influential Factors

Other factors that may have considerable effect on pavement friction include rainfall, pavement age, and traffic. A number of studies have recognized the influence of precipitation on skid resistance. It has been found that the pavement skid resistance decreases during dry periods and increases after rainfall (Dahir et al., 1979). Consequently, some models for predicting long- and short-term seasonal variation

considered the effect of precipitation and number of dry days before the testing. Based on data collected at 21 test sites in Pennsylvania, Hill and Henry (1978) found that there is a weak correlation between SN_{OR} and rainfall and dry days, as shown in Equation 2.22 and Equation 2.23, respectively. Since Dry Spell Factor (DSF), which is the natural logarithm of continuous dry days before the testing day plus the one, shows a better correlation with short-term variations of SN_0 than WRF, DSF was chosen as the parameter of the model (Hill and Henry, 1978).

$$SN_{OR} = 1.00 + 2.74WRF \quad (R^2=0.04) \quad (2.22)$$

$$SN_{OR} = 1.14 + 2.74DSF \quad (R^2=0.12) \quad (2.23)$$

where

WRF = weighted rain factor and

DSF = dry spell factor.

Whitehurst and Neuhardt (1986) observed a decrease in the pavement friction over time on an experimental section in Ohio. Since the test site had only experimental traffic, this decrease was attributed to natural pavement aging. The effect of traffic on skid resistance of pavement is significant, especially under the wheel path. Wambold et al. (1986) showed that the skid number on heavy traffic roads changes dramatically. Traffic polishes the aggregate and reduces the macrotexture of the pavement. Gandhi et al. (1991), Crouch et al. (1995), and Smith and Pollock (1997) also found a significant effect of traffic polishing on microtexture and macrotexture of the pavement surfaces.

2.7 Pavement-Tire Friction Theory

The classical law of friction, first established in the fifteenth century, often has been applied to rubber and rubberlike materials. However, both tire rubber and asphalt pavements are temperature-sensitive materials. Visco-elastic materials, such as rubber, do not completely obey these laws (Kummer and Meyer, 1962). Classical laws of friction state that the friction coefficient is independent of the normal load, the contact area, the sliding velocity, and the temperature, and that the static coefficient is higher than that of

sliding. Research has shown that these statements are not true for viscoelastic materials. For instance, the friction coefficient decreases with increased tire pressure. The friction coefficient between tire and pavement also changes with the slip velocity and temperature. These deviations from the classical laws can be explained by considering adhesion and hysteresis effects.

A specimen of any material sliding on a surface develops a resisting force in the plane of contact. Under specific conditions, this force may be due to a single component, such as adhesive shear or hysteresis (Bowden and Tabor, 1950). However, the mechanism of rubber friction combines both effects as illustrated in Figure 2.3.

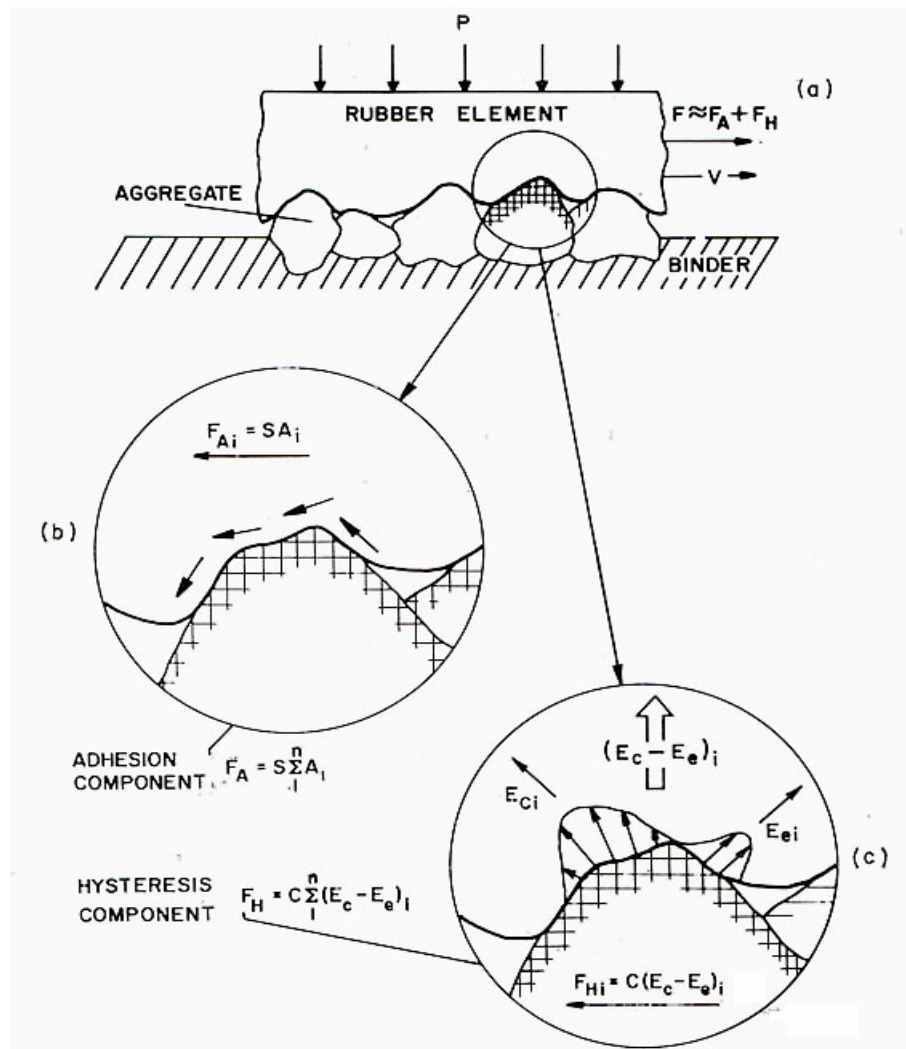


Figure 2.3 Mechanism of Rubber Friction (Kummer and Meyer, 1962)

(Reprinted with permission, copyright ASTM International)

The adhesion component is generated when a single asperity, such as an aggregate particle, penetrates into the rubber block. Due to the quasi-elastic behavior of rubber under compression, high normal pressures (400 to 1000 psi) are developed between the particle and the rubber. Each single interface represents a micro-adhesion component. Shear forces occurring at the molecular interfaces increase with the normal pressure. The summation of the individual shear forces (Equation 2.24) over the dynamic contact area generates a resultant friction shear force F_A as shown Equation 2.25 (Kummer and Meyer, 1962).

$$F_{ai} = sA_{ai} \quad (2.24)$$

$$F_A = s \sum_1^n A_{ai} \quad (2.25)$$

where

F_{ai} = the summation of the individual shear forces;

A_{ai} = actual contact of area at each single rubber and particle interface;

s = shear strength ratio; and

F_A = adhesion component of the tire-pavement friction.

The hysteresis component is more complicated than the adhesion component. When the rubber block moves toward the right (Figure 2.3 c), it must climb over the particle and is subjected to deformation. The deformation consists of a compression phase on the left side of the particle and an expansion phase on the right side. To compress the rubber at the left, an energy quantum E_{ci} is required. At the right side, rubber does not completely return the received energy E_{ci} , but only E_{ei} . The difference between the compression energy and the expansion energy is dissipated in the form of heat. This loss must be compensated for by an outside force F_{Hi} acting in the direction of motion. The outside force F_{Hi} over a single rubber and particle interface is proportional to the energy difference (Equation 2.26).

$$F_{Hi} = c(E_c - E_e)_i \quad (2.26)$$

where

F_{Hi} = the outside force over a single rubber and particle interface;

c = the proportional constant; and
 $(E_c - E_e)_i$ = the Dissipated Heat.

The summation of F_{Hi} over the entire contact area represents the total resistance due to hysteresis F_H (Equation 2.27)

$$F_H = c \sum_1^n (E_c - E_e)_i \quad (2.27)$$

Therefore, the total frictional force (F) can be computed by combining equation 2.26 and 2.27 as shown in Equation 2.28.

$$F = \sum_1^n s(A_a)_i + c(E_c - E_e)_i \quad (2.28)$$

This resultant force represents the tire-pavement friction with acceptable accuracy. Both Meyer (1968) and Tabor (1958) found that the frictional performance of tire rubber is temperature-dependent, and suggested that the heat transformed from the loss of energy of the hysteresis component could warm up tire rubber and change the frictional performance of adhesion and hysteresis components. In addition to the two classical components of friction, Takino et al. (1998) suggested that a cohesion loss term should be considered; this cohesion loss happens when the tire tread rubber is ruptured and torn away from the tire by small asperities, or aggregate roughness, on the pavement surface.

2.8 Summary

Many factors appear to affect long- and short-term fluctuations in the tire-pavement friction. A number of studies showed that temperature changes produce short-term changes in the measured pavement friction. These changes are believed to be partially due to the viscoelastic properties of the tire rubber and hot-mix-asphalt. However, some researchers have obtained contradictory results.

Chapter 3

Experimental Program

The pavement friction research conducted on the Virginia Smart Road is part of a detailed program designed to investigate the surface characteristics of seven different pavement wearing surface mixtures. Details of the pavement friction testing and pavement instrumentation are discussed in following sections.

3.1 The Virginia Smart Road

The Virginia Smart Road testing facility is the first part of a 9.6-kilometer connector highway between Blacksburg and I-81 in southwest Virginia. It has a length of 3.2 kilometers. The facility includes 12 experimental flexible pavement test sections and two rigid pavement sections. The flexible pavement sections are approximately 100-meter long and are being monitored through a complex array of sensors located beneath the roadway and embedded during construction.

Among other features, the pavement test facility includes seven different hot-mix-asphalt (HMA) wearing surfaces: four Superpave mixes with different aggregate structure and binder types, and three experimental mixes. All surface mixes were designed in accordance with the Virginia Department of Transportation Specifications (VDOT 2002). The surface mixture type used in each section and the date of completion for each section are presented in Table 3.1. The surface mix (SM) denomination includes the nominal maximum aggregate size and a letter (A, D, or E), which denotes PG grading of the binder used: PG64-22, 70-22, and 76-22, respectively. The SM-9.5D is the predominant surface mixture type used in Virginia on interstate highways. This type of surface mixture was used on six of the sections. The nominal maximum size (NMS) of the aggregate is defined as one sieve size larger than the first sieve to retain more than 10 percent (Roberts et al., 1996). The HMA surface mix used in section I was designed using 75 gyrations instead of the standard 65 used by VDOT; the (h) stands for “high

compaction.” The two other experimental mixtures are an Open Graded Friction Course (OGFC) and a stone matrix asphalt (SMA-12.5D).

Table 3.1 Wearing Surface Mixes Used at the Virginia Smart Road

Section	Mix	Aggregate NMS	Binder	Completion Date
A	SM-12.5D	9.5 ⁽¹⁾	PG 70-22	11/11/99
B	SM-9.5D	9.5	PG 70-22	11/11/99
C	SM-9.5E	9.5	PG 76-22	11/12/99
D	SM-9.5A	9.5	PG 64-22	11/10/99
E	SM-9.5D	9.5	PG 70-22	11/05/99
F	SM-9.5D	9.5	PG 70-22	11/05/99
G	SM-9.5D	9.5	PG 70-22	11/05/99
H	SM-9.5D	9.5	PG 70-22	11/05/99
I	SM-9.5A(h)	9.5	PG 64-22	11/08/99
J	SM-9.5D	9.5	PG 70-22	11/08/99
K	OGFC	12.5	PG 76-22	11/10/99
L	SMA-12.5D	12.5	PG 70-22	11/09/99

⁽¹⁾ The mix did not meet specification

3.2 Volumetric Properties of the Wearing Surface Mixes

Previous research has shown that volumetric properties of the pavement surface affect the frictional properties of the pavement surface (Huang and Ebrahimzadeh, 1973; Davis, 2001). Thus, the seven wearing surface mixes were tested in the laboratory to determine their HMA design properties. Loose samples were taken during placement of the wearing surface from which specimens were prepared in the laboratory in accordance with VDOT mixture design practices. Gradation analysis, binder content, and specific gravity testing were performed to determine volumetric and composition properties of the mixes. The laboratory results are summarized in Table 3.2. The mixes were produced using a batch plant. Every effort was made to match the design properties. However,

two of the mixes (SM-12.5D and OGFC) failed to meet design specifications. The aggregate gradation for the SM-12.5D was finer than the designed one (9.5 mm NMS), and the OGFC was constructed with a lower asphalt content than the design target.

Table 3.2 Properties of the HMA Wearing Surfaces

	Section	A	B	C	D	E	F	G	H	I	J	L
Volumetrics	Pb	5.9	4.7	5.8	6.3	5.9	5.4	6.3	5.6	5.4	4.9	6.8
	VTM	3.2	3.6	2.3	1.3	1.4	3.6	3.6	4.1	1.5	7.5	1.8
	VMA	16	13	15	15	13	15	17	16	13	17	16
	VFA	80	72	85	91	90	75	79	73	88	55	89
Gradation	19.00	100										100
	12.50	100	98	98	99	98	99	98	98	100	99	99
	9.50	98	90	91	92	93	93	95	94	95	92	88
	4.75	84	52	55	55	63	57	62	64	52	50	37
	2.36	48	35	34	35	43	39	42	43	35	35	25
	1.18	37	27	27	26	32	26	29	29	35	35	21
	0.15	10	9	11	12	10	9	10	10	14	12	14
	0.08	6	8	8	9	8	7	8	8	7	6	11

Pb = percent of asphalt in the mix; VTM = Voids in the Total Mix;
VMA = Voids in the Mineral Aggregate; VFA = Voids Filled with Asphalt.

3.3 Friction Tests

The surface properties were evaluated periodically using different skid resistance and surface macrotexture measuring devices. However, most of the testing was conducted using a locked wheel skid trailer to measure pavement friction, and a laser profiler to measure pavement macrotexture. Since this research investigates the effect of temperature on the skid resistance as measured with the skid trailer (ASTM E 274-97), the main characteristics of this device and the testing procedure are discussed in the following sections.

3.3.1 Locked Wheel Skid Trailer

The locked wheel skid trailer consists of one or more test wheels installed on a suitable trailer towed by a vehicle. The apparatus contains a transducer, instrumentation, a water supply with proper dispensing system, and actuation controls for locking the test wheel. The test wheel is equipped with either a ribbed or a smooth standard pavement test tire (ASTM E-502 and E-524, respectively).

During testing, the skid trailer is brought to the desired test speed. Water is sprayed ahead of the test tire and the braking system is actuated to lock the tire. The resulting friction force acting between the test tire and the pavement surface and the speed of the test vehicle are recorded. The system simulates a 100 percent slip condition, locking the test wheel for one second. The friction force is averaged for the 1 second after the test wheel is fully locked. Therefore, the locked wheel skids over pavement about eight meters at the speed of 32km/hr (20 mph), 18 meters at 64 km/hr (40 mph), and 23 meters at 80 km/hr (50 mph).

The skid test is normally conducted under wet pavement conditions. A standard amount of water is applied right before the test at the tire and pavement interface. The water reduces friction at the interface by lubricating the interface between the tire and the pavement. Meanwhile, it helps control the tire temperature and possibly decreases pavement surface temperature.

The water applied to the pavement ahead of the tire is supplied by a nozzle (Figure 3.1). The quantity of water applied at 64 km/h (40 mph) is 600 ml/min.mm \pm 10% (4.0 gal /min.in \pm 10%) of wetted width. The water layer is at least 25 mm (1 inch) wider than the test tire tread and is applied so the tire is centrally located between the edges. The volume of water per unit lengths is proportional to the test speed (Goodenow, 1967); at higher speed, less water is applied over certain length of pavement. The water jets are directed toward the test tire and pointed toward the pavement at angles of 20° to

30°. The water hits the pavement surface 25 to 46 cm (10 to 18 in) ahead of the center of the wheel axle approximately in 4/1000 second before the wheel.



Figure 3.1 Prewetting System of Skid Trailer

3.3.2 Skid Number Computation

The skid resistance of the paved surface is determined from the measured force or torque and is reported as a skid number (SN). The SN is determined from the force required to slide the locked test tire at a stated speed, divided by the effective wheel load and multiplied by 100. The computerized system computes the skid number using the following equations (ASTM E 274-97).

$$sn(t) = \frac{f_h(t)}{f_v(t)} \times 100 \quad (3.1)$$

$$SN = \frac{1}{t_2 - t_1} \int_{t_1}^{t_2} sn(t) dt \quad (3.2)$$

where

$sn(t)$ = dynamic skid number in real-time;

$f_h(t)$ = dynamic tractive force in real-time, N (or lbf);

$f_v(t)$ = dynamic vertical load in real-time, N (or lbf);

t_1 = time of start of averaging period (s);

t_2 = time of end of averaging period (s); and

SN = mean skid number.

A one-second averaging interval is used under normal operation conditions. Thus, the computer system uses Equation 3.3 to calculate the average SN measured in one second.

$$SN = \int_0^1 sn(t) dt \quad (3.3)$$

Table 3.3 presents an example of raw SN data obtained directly from the skid test trailer collected for section A of the Virginia Smart Road on 3/27/2000. The standard procedure calls for a test speed with $\pm 1.5\%$ allowable speed variation. In addition to the test data, the device records the time of testing. Data from all skid tests are included in Appendix A.

Table 3.3 SN Data for Ribbed Tire Uphill Direction on the Instrumented Lane of Section A

Test ID	Test Time	Test Section	Skid Number (SN)	Standard Deviation of SN	Test Speed	Standard Deviation of Speed
2T-IU-20-1	9:28:30	A	65.3	1.1	18.6	0.1
2T-IU-20-2	9:37:33	A	64	1.8	19.7	0.1
2T-IU-20-3	9:47:24	A	65	2.5	19.2	0.3
2T-IU-40-1	11:02:34	A	50.2	2.2	40.1	0.7
2T-IU-40-2	11:10:35	A	47.8	2.9	40.3	0.1
2T-IU-40-3	11:20:23	A	48.8	2.5	40.3	0.2
2T-IU-60-1	12:35:43	A	43.2	2.6	49.6	0.4
2T-IU-60-2	12:44:00	A	39	3.6	53.4	0.3
2T-IU-60-3	12:50:45	A	43.8	4.9	50.2	0.3

3.3.3 Calibration of Locked Wheel Skid Trailer

Periodic calibration of the locked wheel skid trailer is required to assure the accuracy of the measured data. The standard procedure to calibrate the skid trailer and control the variation of test results includes calibration of the speedometer and calibration of the skid resistance force gauge (ASTM E 274-97). The vehicle speed measuring transducer shall provide speed resolution and accuracy of $\pm 1.5\%$ of the intended speed or ± 0.8 km/h (± 0.5 mph). The force and torque measuring transducers shall provide an output directly proportional to force, with hysteresis less than 1% of the applied load. Therefore, the overall system accuracy is approximately $\pm 1.5\%$ of the applied load.

3.3.4 Testing Program

Periodic tests using the ribbed and smooth tires were conducted. The test program began on March 2000 and ended on August 2002. During the two and a half years of testing, six sets of tests were conducted with each tire. Each test set included tests at the three target speeds, on both lanes and in both directions (uphill and downhill). Three repetitions were conducted for each lane, direction, and target speed. The dates and times of all tests are presented in Table 3.4.

Table 3.4 Time Information of Skid Tests

Test	Date	From	To	Tire
1B	03/09/00	8:53	13:46	Smooth
4B	10/04/00	12:39	16:13	Smooth
5B	02/07/01	9:05	12:03	Smooth
6B	09/25/01	8:11	11:37	Smooth
7B	05/01/02	7:07	11:18	Smooth
8B	08/06/02	8:25	11:12	Smooth
2T	03/27/00	9:22	13:28	Ribbed
3T	09/19/00	14:02	19:00	Ribbed
5T	02/07/01	13:56	16:30	Ribbed
6T	10/03/01	7:44	11:06	Ribbed
7T	05/01/02	7:07	11:18	Ribbed
8T	08/06/02	11:41	13:08	Ribbed

A coding system was used to identify the skid measurements, according to which each test is identified based on the test sequence, speed, lane, and grade. The first digit in the code indicates the test sequence. The letter in the second position indicates the type of tire used, B for the smooth tire and T for the ribbed tire. The letter in the third position refers to the lane in which the test was conducted, I for instrumented and N for non-instrumented. The letter in the fourth position indicates the direction (grade) in which the tests were run, U for uphill and D for downhill. The following two digits denote the target speed 32, 64, or 80 km/hr (20, 40, or 50 mph). The last digit indicates the repetition number. For example, the code 1B-IU-20-1 denotes the first repetition for the first test (conducted in March 2000) using smooth tire (B) at a speed of 32 km/hr (20 mph) on the instrumented lane and uphill direction (IU).

3.4 Pavement Temperature

T-shape thermocouples (Figure 3.2) were used at the Virginia Smart Road to measure pavement temperature because of their accuracy, service life, field installation, and price. The thermocouples were embedded in the pavement during construction. All thermocouples are connected to a computer monitoring system. The computer monitoring system automatically collects the temperature data of each layer in all sections every 15 minutes (Al-Qadi et al., 2000).



Figure 3.2 T-shape Thermocouple

The thermocouples were calibrated using hot and cold water baths to determine their accuracy at extreme temperatures. It was determined that all the thermocouples performed with acceptable accuracy ($\pm 1^{\circ}\text{C}$). In addition, all thermocouples were checked after construction for sway in reading and accuracy, using a hand-held T-shape Thermocouple Meter (Diefenderfer, 2000).

3.4.1 Pavement Temperature Measurements

To study the effect of pavement temperature on pavement friction, it was necessary to obtain the pavement temperature using the date and time of each test. Since each single test has a certain time stamp, the corresponding temperature can be obtained from the real-time temperature monitoring system. Table 3.5 shows an example of the pavement temperature measured on each section for three consecutive tests at 32 km/h (20 mph) on 9/25/2002. For example, 6B-ID-20-1 was conducted at 10:21AM on section A, which corresponds to the temperature of 17.5 °C at 10:15 AM in the temperature data file. The pavement temperatures during all tests are included in Appendix B.

Table 3.5 Example of Measured Pavement Temperature

Section	Test		
	6B-ID-20-1	6B-ID-20-2	6B-ID-20-3
	10:21	10:28	10:36
A	17.5	17.8	18.0
B	16.5	16.8	17.1
C	16.1	16.4	16.6
D	17.7	18.0	18.4
E	16.8	17.1	17.4
F	18.8	19.2	19.5
G	17.7	18.0	18.4
H	17.4	17.8	18.1
I	18.2	18.5	18.9
J	15.9	16.2	16.5
K	13.3	13.4	13.4
L	11.6	11.9	12.2

3.4.2 Pavement Temperature Verification Tests

Additional tests were conducted to assess the impact of the sprayed water on pavement temperature. It was suspected that water applied during testing may cool down both tire and pavement surface. Since the thermocouples are not located exactly under the testing locations, this effect is not measured. Therefore, the effect of water on pavement temperature was investigated using three types of pavements. Tests were conducted on sunny and cloudy days. A thin film of water was applied over selected pavement spots on an outdoor basketball court, a parking lot, and a local street road. Temperatures of water and pavement were measured right before applying water, immediately after applying the water, and every 10 or 15 minutes thereafter. Data was also collected one to two hours after applying the water to see the prolonged effect.

Chapter 4

Data Collection and Analysis

This chapter presents the data collection and analysis for the experimental program designed to establish the effect of pavement temperature on the pavement frictional properties.

4.1 Data Collection

Two main types of data were analyzed for this investigation: pavement friction measurements and pavement temperature. In addition, the properties of the HMA wearing surface investigated were determined using laboratory tests.

4.1.1 Pavement Friction Measurements

As indicated in Chapter 3, the pavement friction data were obtained using a locked wheel skid trailer. The tests were conducted at three different speeds, 32, 64, and 80 km/hr (20, 40, and 50mph), using both the ribbed and the smooth tires. Figures 4.1 and 4.2 show the average test results for the instrumented lane of the experimental sections measured at the three target testing speeds for the different testing dates. It can be observed that, as expected, the friction measurements with the ribbed tire are less sensitive to speed than those measured with the smooth tire. The measurements with the smooth tire also appear to be more sensitive to environmental changes since they experience more variations from test to test. All test results are included in Appendix A. The first test using each tire were not included in the analysis because the temperature monitoring system was not yet operational at the time of the tests. Thus, no accurate temperature measurements were available for this investigation.

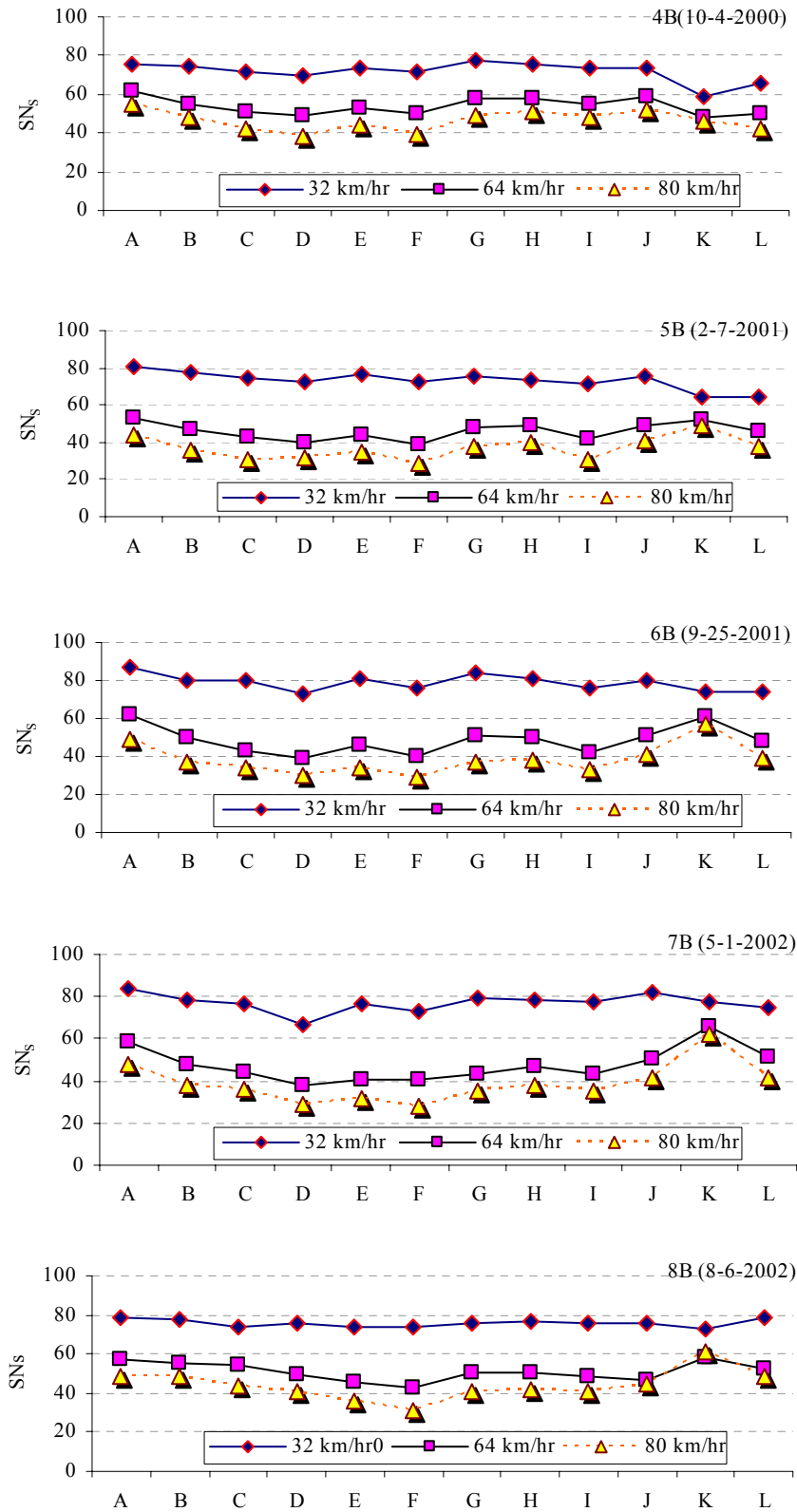


Figure 4.1 Average Skid Numbers Measured Using the Smooth Tire (SN_s)

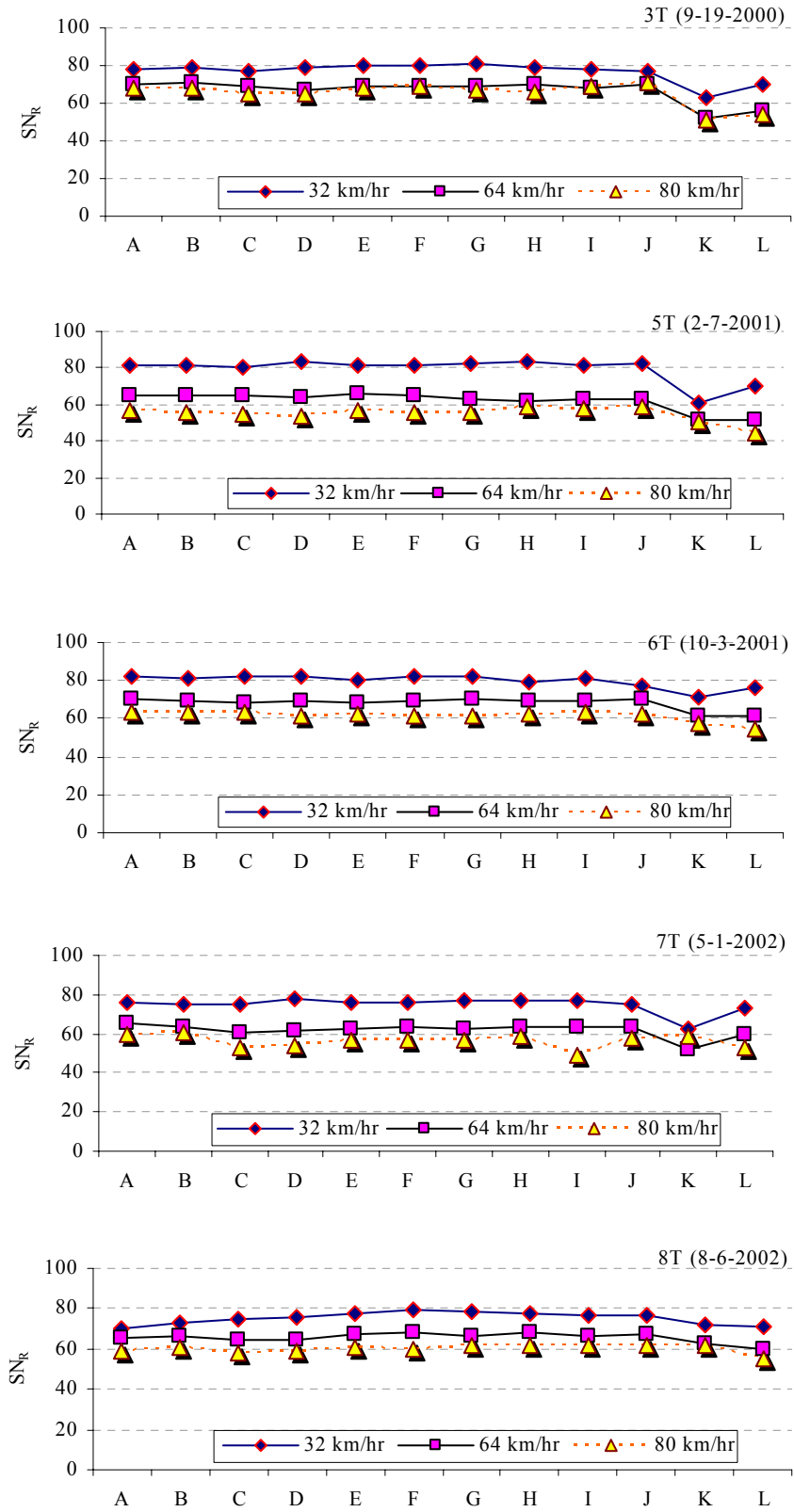


Figure 4.2 Average Skid Numbers Measured Using the Ribbed Tire (SN_R)

4.1.2 Temperature Data

The real time temperature monitoring system collects the pavement surface temperature every 15 minutes from the thermocouples laid in the wearing surface layer. The thermocouples were labeled as follows: the first letter denotes the pavement section; the second letter (T) denotes the type of instrument (thermocouple); the first number denotes the layer (1 for the wearing surface, 2 for the base layer, etc.); the second number (1 or 2) denotes the number of the thermocouple in the layer; and the last letter denotes the location of the thermocouple (B indicates that it is placed at the bottom of the layer, and T at the top). Table 4.1 presents an example of the temperature monitoring system output for the thermocouples placed in section B. The last three columns correspond to the measurements in the HMA base course. The average of the thermocouples placed at the bottom of the wearing surface was used as the pavement temperature in the analysis (e.g., BT-1B and BT-2B in the example presented in Table 4.1).

Table 4.1 Example Output of the Temperature Monitoring System for Section B

Time	Thermocouples (°C)						
	BT1-1B	BT1-2B	Pavement Temp.	ABT0	BT2-2B	BT2-1T	BT2-2T
3/24/00 08:33	12.3	12.0	12.2	18.0	11.9	14.4	13.2
3/24/00 08:48	13.6	13.5	13.6	20.5	12.1	14.3	13.4
3/24/00 09:04	14.8	14.4	14.6	28.9	12.3	14.2	13.8
3/24/00 09:19	16.2	16.0	16.1	29.0	12.5	14.9	14.6
3/24/00 09:41	17.3	16.7	17.0	27.9	12.9	15.5	14.4
3/24/00 10:02	18.9	18.0	18.5	26.7	12.2	14.6	14.5
3/24/00 10:17	20.2	19.0	19.6	23.9	12.2	14.7	14.0
3/24/00 10:32	22.0	20.9	21.5	26.8	12.6	16.0	15.4
3/24/00 10:47	23.0	21.9	22.5	23.9	13.1	16.0	15.2
3/24/00 11:03	22.7	22.5	22.6	32.0	14.0	17.0	16.0
3/24/00 11:18	25.3	23.1	24.2	30.2	13.7	17.6	16.9

Figure 4.3 shows the progression of the temperature in a typical day for section B. The figure shows that pavement temperature changes lag behind those in air temperature near pavement surface (ABT0). For example, the maximum temperature in the wearing surface occurs approximately 2.5 hours after the maximum air temperature. It is also noted that the measurements of the two thermocouples in the wearing surface (BT1-1B and BT1-2B) are very close.

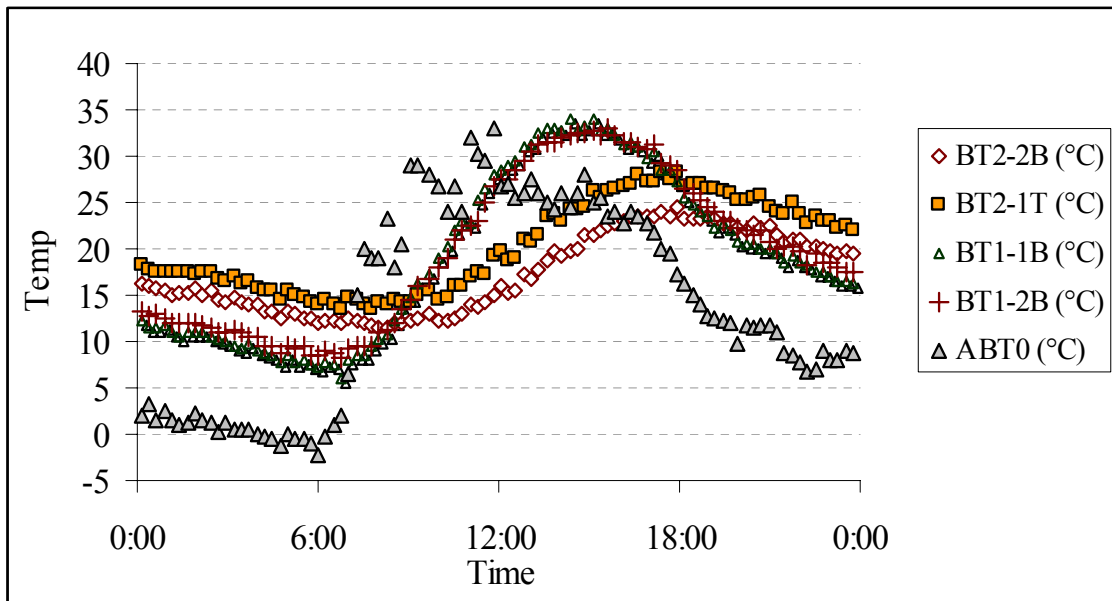


Figure 4.3 Pavement Temperature Profile for Section B in a Typical Day

The pavement temperature data in the wearing surface layer were obtained for each of the skid tests conducted and obtained in a database. The average pavement temperatures during all the skid tests are presented in Table 4.2. The temperatures for all individual tests are included in Appendix B.

Table 4.2 Average Pavement Temperature (°C) 38 mm below Surface for All Tests

Section	Tests Using Smooth Tire						Tests Using Ribbed Tire					
	1B	4B	5B	6B	7B	8B	2T	3T	5T	6T	7T	8T
A	26.0	37.3	10.2	17.1	21.4	33.6	25.8	35.9	18.2	20.6	30.6	44.3
B	23.9	36.3	8.8	16.3	20.4	32.7	24.9	34.4	17.4	19.7	32.0	38.6
C	23.7	36.4	9.7	15.3	20.7	21.9	19.0	34.5	16.6	19.0	26.8	33.3
D	22.0	36.4	9.6	17.3	21.2	27.2	18.2	35.3	18.5	20.0	31.1	34.9
E	21.8	35.6	9.6	16.2	19.9	32.5	29.5	34.3	16.1	18.3	28.6	44.7
F	21.8	39.2	11.7	18.5	21.8	34.4	29.8	37.2	18.8	20.7	31.4	42.2
G	21.8	39.3	11.7	17.2	20.7	33.9	29.7	36.0	20.5	20.1	31.4	46.0
H	21.8	37.9	11.1	17.1	20.6	33.7	29.7	36.8	19.3	19.7	31.8	45.5
I	10.3	39.6	12.4	17.7	18.3	44.8	24.5	37.8	20.5	21.2	32.5	49.3
J	12.3	36.2	9.3	15.5	16.8	46.5	25.2	34.6	17.6	19.2	30.5	51.1
K	12.8	28.4	2.0	12.9	18.9	32.7	26.0	29.7	11.6	16.1	22.6	36.0
L	12.3	32.9	11.4	10.9	20.5	34.3	26.9	38.3	20.0	16.1	31.0	43.9

4.2 Data Analysis

The analysis of the effect of pavement temperature on pavement friction included three steps. The first step consisted of conducting a regression analysis for each target testing speed using all tests, but considering the measurements using the smooth and ribbed tires separately. Secondly, the results were verified using selected tests. Finally, the parameters of the Penn State model were computed and the effect of temperature on these parameters was analyzed.

4.2.1 Regression Analysis

The first step in the analysis consisted of a regression analysis using all pavement friction data at each target testing speed. The correlation between pavement friction and pavement temperature was studied separately for the measurements obtained using the smooth and ribbed tires. It was suspected that the two types of tires could have difference frictional response to the change of pavement temperature. The friction data used in the analysis are the raw SN data collected at the three testing speeds: 32, 64 and 80 km/hr (20, 40 and 50 mph), denoted as SN₂₀, SN₄₀, and SN₅₀, respectively. The

measured SN at a specific speed was considered the dependent variable and the corresponding pavement temperatures as the independent variable.

4.2.1.1 SN_S Analysis

The measurements using smooth tire were expected to be more sensitive to temperature than those obtained using the ribbed tire because of the more significant variability observed in Figure 4.1. In order to have a large number of measurements, the initial analysis was conducted combining the friction data collected on sections E through H (Figure 4.4). These sections have the same wearing surface mix and were constructed at the same time. The data from the first test (1B) was excluded from the analysis because the temperature monitoring system was not operational at the time of testing and thus only an estimate temperature was available. The results of regression analysis for the measurements at the three target testing speeds are summarized in Table 4.3.

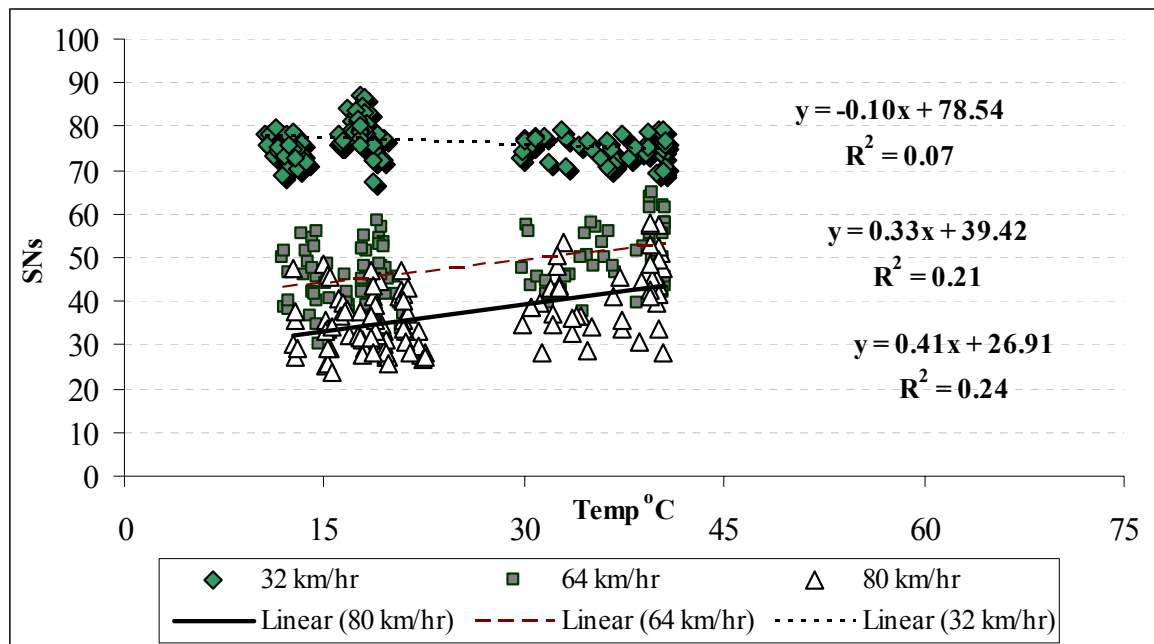


Figure 4.4 SN_S versus Pavement Temperature for Sections E through H

Table 4.3 SN_s Regression Analysis Results (Sections E through H)

	Slope	Intercept	R ²	Prob.> t	RMSE
SN _{S20}	-0.1	78.54	0.07	0.3615	3.32
SN _{S40}	0.33	39.42	0.21	0.0002	6.45
SN _{S50}	0.41	26.91	0.24	0.0001	6.89

Although it must be noted that the correlations in all cases are weak at best, the results presented in Table 4.3 indicate that SN_{S40} and SN_{S50} tend to increase with increased pavement temperature. Conversely, no significant effect of pavement temperature on SN_{S20} was observed.

To verify if the trend observed for the standard mix was also observed for the other mixes, a similar regression analysis was conducted for all individual pavement sections. The results of regression analysis for the skid tests on sections A through L are presented in Table 4.4.

Table 4.4 SN_s Regression Analysis Results for All Individual Sections

Section	Mix Type	SN _{S20} (32 km/hr)			SN _{S40} (64 km/hr)			SN _{S50} (80 km/hr)		
		Slope	Inter.	R ²	Slope	Inter.	R ²	Slope	Inter.	R ²
A	SM-12.5D	-0.30	73.72	0.47	0.35	35.00	0.07	0.53	32.25	0.66
B	SM-9.5D	-0.19	83.65	0.32	0.27	44.23	0.02	0.49	30.50	0.46
C	SM-9.5E	-0.18	79.16	0.15	0.32	39.95	0.34	0.49	27.00	0.31
D	SM-9.5A	-0.11	76.00	0.02	0.37	38.30	0.35	0.32	30.00	0.43
E	SM-9.5D	-0.17	80.25	0.25	0.32	38.85	0.24	0.33	28.31	0.18
F	SM-9.5D	-0.09	75.83	0.12	0.35	33.38	0.32	0.39	21.05	0.39
G	SM-9.5D	-0.10	80.80	0.23	0.38	40.96	0.35	0.52	26.67	0.61
H	SM-9.5D	-0.19	82.90	0.51	0.29	43.96	0.23	0.38	31.55	0.22
I	SM-9.5A(h)	-0.06	77.19	0.08	0.21	41.60	0.26	0.40	26.60	0.58
J	SM-9.5D	-0.09	77.20	0.04	0.31	42.00	0.40	0.56	25.00	0.70
K	OGFC	0.24	62.35	0.07	0.11	52.10	0.01	0.22	50.00	0.08
L	SMA-12.5D	0.10	70.00	0.26	0.21	46.00	0.16	0.41	32.70	0.44

The table shows that the results are not consistent for all sections, indicating that the dependence of SN_S on pavement temperature may be mix-dependent. In general, for the finer mix, the friction measurements at 32 km/hr (20mph) tend to slightly decrease, and the measurements conducted at higher speed tend to slightly increase with higher temperatures. However, as in the previous case, all the coefficients of determination are very low. The measurements on the OGFC (Section K) do not seem to be affected by temperature.

4.2.1.2 SN_R Analysis

A similar analysis was conducted for the measurements obtained using the ribbed tire. The analysis used the combined friction measurements obtained on sections E through H. Figure 4.5 shows the trends at the three target speeds. The results of the regression analysis are summarized in Table 4.5. While SN_{R20} is weakly correlated with pavement temperature (tend to decrease with higher temperature), SN_{R40} and SN_{R50} do not seem to be significantly affected by temperature.

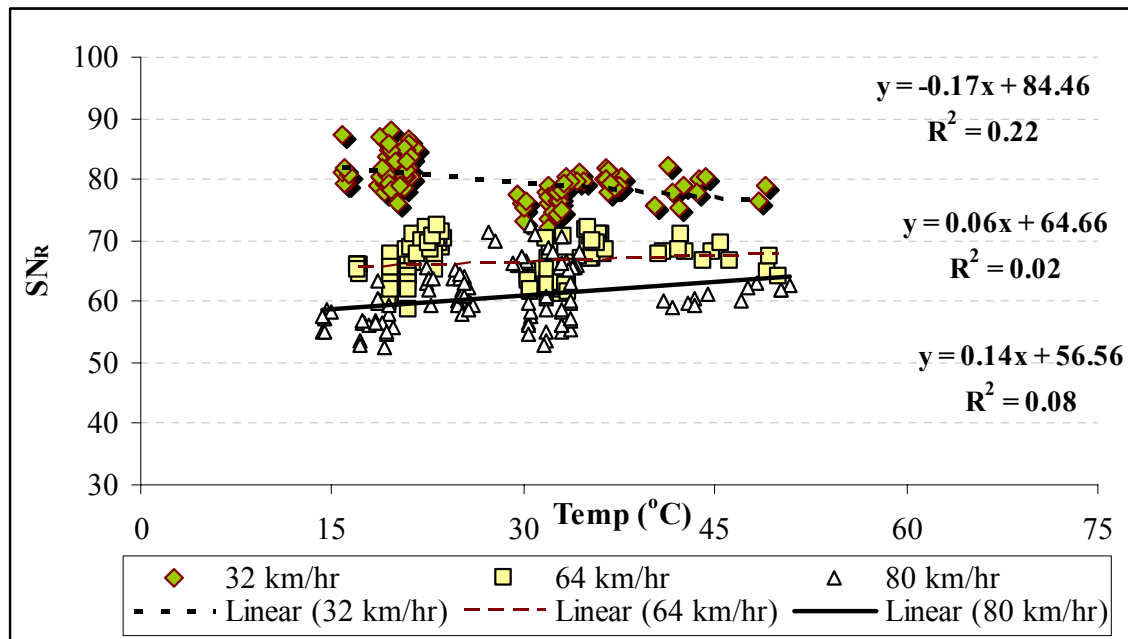


Figure 4.5 SN_R versus Pavement Temperature for Sections E through H

Comparing to Figure 4.4, reverse effect was observed for ribbed tire: SN_{R20} was negatively correlated with pavement temperature while no correlations were found for SN_{R40} and SN_{R50} . This effect could happen due to the factual differences of surface condition among sections E through H.

Table 4.5 SN_R Regression Analysis Results (Sections E through H)

	Slope	Intercept	R²	Prob.> t 	RMSE
SN_{R20}	-0.17	84.46	0.22	0.002	2.72
SN_{R40}	0.06	64.66	0.02	0.36	3.31
SN_{R50}	0.14	56.56	0.08	0.172	4.43

To determine if the conclusions are mix-specific, the regression analysis was also conducted for each section individually. The results are summarized in Table 4.6. Similar trends were observed in most cases; however, the results are not consistent for all the sections. Again the OGFC (Section k) showed a different behavior since it is not affected by temperature changes. For most mixes, there is indication of that the measurements at 80 km/hr may have a positive correlation with speed.

Table 4.6 SN_R Regression Analysis for All Individual Sections

Section	SN_{R20} (2 km/hr)			SN_{R40} (64 km/hr)			SN_{R50} (80 km/hr)		
	Slope	Interc.	R²	Slope	Interc.	R²	Slope	Interc.	R²
A	-0.38	84.35	0.59	0.09	65.15	0.10	0.16	59.80	0.14
B	-0.32	87.15	0.54	0.01	70.12	0.01	0.37	50.41	0.33
C	-0.30	85.46	0.39	0.03	64.72	0.01	0.23	55.59	0.07
D	-0.34	89.47	0.52	-0.12	68.41	0.06	0.26	51.59	0.12
E	-0.13	78.58	0.23	-0.03	63.50	0.01	0.14	54.47	0.07
F	-0.13	89.39	0.26	0.05	68.59	0.04	0.34	51.79	0.17
G	-0.19	85.91	0.34	0.00	62.68	0.01	0.28	53.84	0.24
H	-0.19	89.49	0.39	0.08	61.28	0.16	0.11	58.27	0.05
I	-0.19	89.1	0.34	0.06	60.90	0.02	0.19	55.08	0.08
J	-0.13	81.72	0.19	0.09	64.44	0.03	0.18	60.76	0.04
K	0.10	68.81	0.02	0.04	53.44	0.05	0.11	71.04	0.07
L	-0.15	76.11	0.18	0.05	58.80	0.04	0.32	44.91	0.27

4.2.1.3 Model Verification

Two tests that were conducted within a short period of time but under different environmental conditions were compared to verify the previous findings. This allowed for observing the effect of temperature independent of other time-related factors, such as age and traffic. Therefore, the two contiguous tests with the largest pavement temperature difference were selected for the friction measurements using the smooth and ribbed tires:

- Tests 4B , conducted in October 2000 with an average pavement temperature of 37.8°C (100°F), and 5B, conducted in February 2002 with an average pavement temperature of 10°C (50 °F) for SN_S, and
- Tests 3T, conducted in September 2000 with an average pavement temperature of 35.5°C, and 5T, conducted in February 2001 with an average temperature of 17.9°C for SN_R.

Table 4.7 presents the results of the linear regression analysis using only tests 4B and 5B and Table 4.8 presents the results of the regression analysis using only tests 3T and 5T.

Table 4.7 SN_S Regression Analysis Results Using Two Testing Dates (4B and 5B)

Test Section	SN _{S20} (32 km/hr)			SN _{S40} (64 km/hr)			SN _{S50} (80 km/hr)		
	Slope	Interc.	R ²	Slope	Interc.	R ²	Slope	Interc.	R ²
A	-0.31	86.83	0.95	0.43	44.73	0.86	0.61	32.41	0.98
B	-0.22	76.95	0.51	0.32	46	0.8	0.65	29.64	0.92
C	-0.12	79.01	0.53	0.42	39.7	0.84	0.5	27.99	0.91
D	-0.06	77.99	0.61	0.42	41.96	0.88	0.39	31.15	0.77
E	-0.04	74.82	0.03	0.46	33.28	0.97	0.5	22.59	0.8
F	-0.07	74.09	0.13	0.38	28.49	0.84	0.38	19.23	0.6
G	0.18	70.93	0.83	0.56	35	0.9	0.5	27.06	0.88
H	0.08	71.46	0.21	0.29	41.1	0.7	0.54	23.95	0.9
I	-0.01	72.46	0.01	0.34	39.07	0.65	0.58	23.42	0.82
J	0.04	71.68	0.08	0.37	37.56	0.84	0.56	25.83	0.86
K	-0.19	67.02	0.7	-0.15	53.22	0.73	-0.11	51.11	0.59
L	0.1	63.46	0.15	0.07	47.42	0.16	0.16	37.92	0.22

Table 4.8 SN_R Regression Analysis Results Using Two Testing Dates (3T and 5T)

Test Section	SN _{R20} (32 km/hr)			SN _{R40} (64 km/hr)			SN _{R50} (80 km/hr)		
	Slope	Interc.	R ²	Slope	Interc.	R ²	Slope	Interc.	R ²
A	-0.18	85.03	0.65	0.31	59.00	0.56	0.78	43.82	0.77
B	-0.09	82.63	0.08	0.38	58.25	0.69	0.79	43.32	0.84
C	-0.16	82.80	0.56	0.27	59.95	0.65	0.64	44.43	0.66
D	-0.28	89.20	0.71	0.21	60.13	0.40	0.71	41.10	0.70
E	-0.09	83.00	0.13	0.21	61.88	0.55	0.72	46.74	0.86
F	-0.11	83.74	0.24	0.30	58.57	0.57	0.90	39.89	0.88
G	-0.15	86.08	0.31	0.42	53.77	0.74	0.75	41.24	0.90
H	-0.28	88.95	0.49	0.48	52.86	0.85	0.50	49.73	0.71
I	-0.16	84.56	0.21	0.37	54.53	0.63	0.77	43.06	0.72
J	-0.29	87.26	0.52	0.48	54.33	0.75	0.86	44.69	0.71
K	0.10	60.02	0.08	-0.02	52.21	0.01	0.02	50.63	0.02
L	-0.07	73.24	0.13	0.29	45.41	0.53	0.61	32.48	0.80

The result presented in tables 4.7 and 4.8 in general agree with those obtained using all tests. It must be noted that although the coefficients of determination for the regressions are higher, there are only two temperature sets in each case.

4.2.2 Temperature Effect on SN₀ and PNG

The effect of temperature on the parameters of the Penn State Model was also analyzed to better understand the pavement temperature effect on the overall pavement frictional properties. This analysis also helped explain some of the contra-intuitive findings obtained in the previous sections. Each individual data set, comprised of three tests at each target speed on a particular section lane and direction, was used to compute an SN₀ and PNG pair. These parameters were obtained by fitting an exponential curve to the data. Very good coefficients of determination were obtained in all cases. Figure 4.6 shows an example; it presents the model obtained for the fifth uphill test (U) on the instrumented lane (I) of section A using the smooth tire (B). In this case, SN₀ is 132.1, and PNG is 2.0 hr/km. The calculated SN₀ and PNG values have been proven to be related to the surface microtexture and macrotexture, respectively. SN₀ is mostly affected

by the surface microtexture, and PNG is inversely proportional to the surface macrotexture.

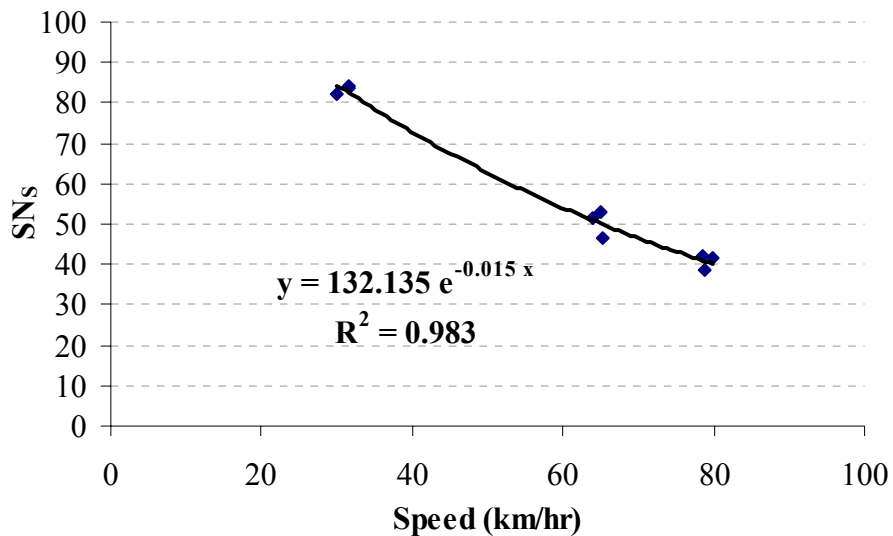


Figure 4.6 Exponential Regression for the Section A Test Set 5B-IU

The first set of tests using each tire (1B and 2T) were not included in the analysis because the temperature monitoring system was not fully operational at the time of testing. Thus, no accurate temperature data was available.

4.2.2.1 Smooth Tire Measurements

The Penn State Model parameters computed for the measurements on sections E through H and the average pavement temperature (T_p) during each set of tests are presented in Table 4.9. To minimize the effect of other variables, only the measurements on the instrumented lane obtained for the uphill direction were used for this analysis. Table 4.9 presents the averaged pavement temperatures (T_p) in $^{\circ}\text{C}$ and the SN_0 and PNG calculated for the tests using the smooth tire on the uphill direction of the instrumented section (B-IU) for the four sections. Figure 4.7 shows the general trends of change of SN_{s0} and PNG with pavement temperature. Although the coefficients of determination for the linear regressions obtained are not very good, a negative correlation can be observed.

Table 4.9 Calculated SN_{S0} and PNG (hr/km) for Sections E through H

Section	Parameter	1B	4B	5B	6B	7B	8B
E	T_p ($^{\circ}C$)	21.7	35.9	9.3	16	19.9	32.7
	SN_0	110.8	105.2	141.8	149	148.2	124.6
	PNG	1.5	1.2	2.0	2.0	2.0	1.6
	R^2	0.91	0.95	0.99	0.97	0.99	1
F	T_p ($^{\circ}C$)	21.7	39.2	11.4	18.3	21.8	34.6
	SN_0	109.1	115.3	149.6	141.3	156.1	128.2
	PNG	1.6	1.6	2.2	2.1	2.2	1.7
	R^2	0.88	0.92	0.99	0.97	0.97	1
G	T_p ($^{\circ}C$)	21.7	37.8	11.4	16.9	20.8	34.1
	SN_0	138.7	109.2	117.8	142	145.5	114
	PNG	1.8	1.1	1.5	1.6	1.8	1.3
	R^2	0.97	0.97	0.98	0.94	0.97	0.9
H	T_p ($^{\circ}C$)	21.7	37.8	10.8	16.9	20.6	33.6
	SN_0	118.8	103.4	122.8	149.7	153.3	118.5
	PNG	1.6	1.1	1.7	1.9	1.9	1.3
	R^2	0.97	0.97	0.97	0.93	0.96	1

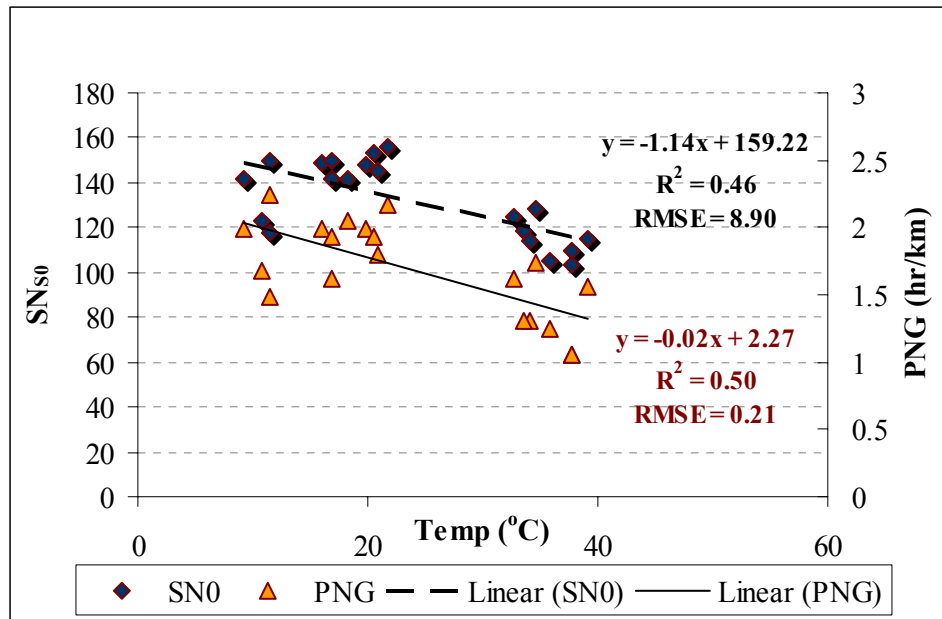


Figure 4.7 SN_{S0} and PNG versus Pavement Temperature for Sections E through H

Table 4.10 summarizes the regression analysis results for all the sections. Except for section K, there is mild to strong negative correlation of SN_{s_0} and PNG with the pavement temperature, indicating that both parameters tend to decrease with a higher temperature. This finding is consistent with the analysis of the measurements at the various speeds as discussed later in this chapter.

Table 4.10 SN_{s_0} and PNG (hr/km) Regression Analysis Results for All Sections

Test Section	SN_{s_0}				PNG (hr/km)			
	Obs.	Slope	Interc.	R^2	Obs.	Slope	Interc.	R^2
A	5	-0.85	131	0.21	5	-0.025	1.21	0.25
B	5	-1.15	129.5	0.67	5	-0.022	1.58	0.82
C	5	-1.08	124.6	0.6	5	-0.025	1.58	0.95
D	5	-0.95	127.1	0.39	5	-0.022	1.52	0.79
E	5	-1.42	166	0.73	5	-0.024	2.46	0.81
F	5	-1.22	169	0.74	5	-0.025	2.59	0.93
G	5	-0.86	147.8	0.3	5	-0.028	1.95	0.61
H	5	-1.15	157	0.38	5	-0.033	2.16	0.68
E - H	20	-1.14	159.2	0.46	20	-0.024	2.27	0.5
I	5	-1.21	138.1	0.39	5	-0.032	1.6	0.68
J	5	-1.24	125.6	0.41	5	-0.025	1.65	0.83
K	5	-0.13	172.2	0.03	5	0.002	0.5	0.01
L	5	-0.45	103.6	0.29	5	-0.014	1.07	0.67

4.2.2.2 Ribbed Tire Measurements

A similar analysis was conducted for the friction measurements using the ribbed tire. The parameters of the Penn State Model, SN_{R0} and PNG, were determined using regression analysis for each friction test set. The results for sections E through H are presented in Table 4.11 and Figure 4.8. Figure 4.8 shows that as in the case of the smooth tire, both parameters tend to decrease with increased temperature. However, the observed effect on both PNG and SN_{R0} using ribbed tire is smaller than for that using the smooth tire.

Table 4.11 Calculated SN_{R0} and PNG (hr/km) for Sections E through H

Section	Parameter	2T	3T	5T	6T	7T
E	T_p ($^{\circ}C$)	25.80	37.40	16.00	18.40	29.10
	SN_{R0}	86.50	89.50	105.40	98.40	94.70
	PNG	0.76	0.42	0.75	0.61	0.64
	R^2	0.97	0.96	0.93	0.98	0.93
F	T_p ($^{\circ}C$)	25.80	39.90	19.20	20.80	31.40
	SN_{R0}	87.40	86.50	107.30	105.20	100.20
	PNG	0.82	0.29	0.82	0.66	0.72
	R^2	0.93	0.97	0.95	0.93	0.99
G	T_p ($^{\circ}C$)	25.80	37.90	19.60	20.20	31.30
	SN_{R0}	92.80	92.20	109.70	101.20	98.10
	PNG	0.93	0.42	0.85	0.60	0.68
	R^2	0.92	0.94	0.97	0.97	0.95
H	T_p ($^{\circ}C$)	25.80	38.90	20.70	19.80	30.80
	SN_{R0}	96.30	89.30	110.30	95.80	94.60
	PNG	0.98	0.39	0.83	0.48	0.54
	R^2	0.97	0.97	0.95	0.92	0.98

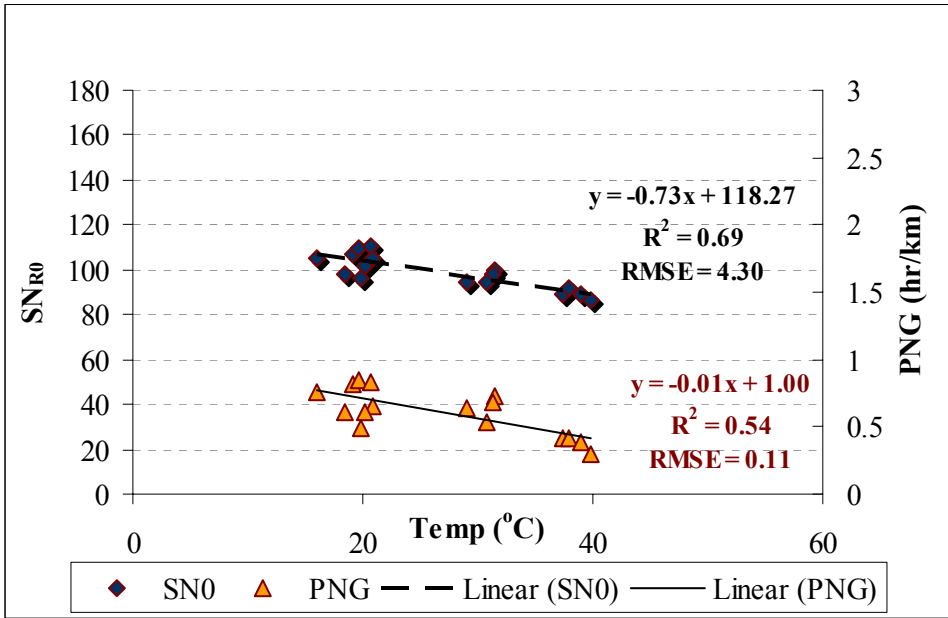


Figure 4.8 SN_{R0} and PNG versus Pavement Temperature for Sections E through H

4.2.2.3 Model Verification

The results presented in the previous sections indicate that both the pavement friction at zero speed (SN_0) and the gradient of friction with speed (PNG) decrease with increased pavement temperature. However, SN_0 and PNG were determined using test at three speeds that were conducted over a certain range of temperatures and the average for that range was considered in the analysis. To verify that this did not have a significant effect on the findings, the trend was verified by correcting SN_{20} , SN_{40} and SN_{50} to three standard temperatures and then determining the SN_0 and PNG at these three temperatures.

The values of SN_{20} , SN_{40} and SN_{50} at 0, 25 and 50°C were computed from all pavement sections based on the linear models presented in Tables 4.4 and 4.6. The results are presented in Tables 4.12 and 4.13, for the smooth and ribbed tires respectively. Exponential models were then fitted to the data to determine the Penn State Model parameters at the three temperatures. As an example, the models determined for sections E through H combined at three temperatures for both the smooth and ribbed tires are depicted in Figures 4.9 and 4.10, respectively.

Table 4.12 Calculated SN_s for All Sections at 0, 25 and 50°C

Section	Calculated SN_{S20}			Calculated SN_{S40}			Calculated SN_{S50}		
	0°C	25°C	50°C	0°C	25°C	50°C	0°C	25°C	50°C
A	73.7	66.2	58.7	35.0	43.8	52.5	32.3	45.5	58.8
B	83.7	78.9	74.2	44.2	51.0	57.7	30.5	42.8	55.0
C	79.2	74.7	70.2	40.0	48.0	56.0	27.0	39.3	51.5
D	76.0	73.3	70.5	38.3	47.6	56.8	30.0	38.0	46.0
E	80.3	76.0	71.8	38.9	46.9	54.9	28.3	36.6	44.8
F	75.8	73.6	71.3	33.4	42.1	50.9	21.1	30.8	40.6
G	80.8	78.3	75.8	41.0	50.5	60.0	26.7	39.7	52.7
H	82.9	78.2	73.4	44.0	51.2	58.5	31.6	41.1	50.6
I	77.2	75.7	74.2	41.6	46.9	52.1	26.6	36.6	46.6
J	77.2	75.0	72.7	42.0	49.8	57.5	25.0	39.0	53.0
K	62.4	68.4	74.4	52.1	54.9	57.6	50.0	55.5	61.0
L	70.0	72.5	75.0	46.0	51.3	56.5	32.7	43.0	53.2

Table 4.13 Calculated SN_R for All Sections at 0, 25 and 50°C

Section	Calculated SN _{R20}			Calculated SN _{R40}			Calculated SN _{R50}		
	0°C	25°C	50°C	0°C	25°C	50°C	0°C	25°C	50°C
A	84.4	74.9	65.4	65.2	67.4	69.7	59.8	63.8	67.8
B	87.2	79.2	71.2	70.1	70.4	70.6	50.4	59.7	68.9
C	85.5	78.0	70.5	64.7	65.5	66.2	55.6	61.3	67.1
D	89.5	81.0	72.5	68.4	65.4	62.4	51.6	58.1	64.6
E	78.6	75.3	72.1	63.5	62.8	62.0	54.5	58.0	61.5
F	89.4	86.1	82.9	68.6	69.8	71.1	51.8	60.3	68.8
G	85.9	81.2	76.4	62.7	62.7	62.7	53.8	60.8	67.8
H	89.5	84.7	80.0	61.3	63.3	65.3	58.3	61.0	63.8
I	89.1	84.4	79.6	60.9	62.4	63.9	55.1	59.8	64.6
J	81.7	78.5	75.2	64.4	66.7	68.9	60.8	65.3	69.8
K	68.8	71.3	73.8	53.4	54.4	55.4	71.0	73.8	76.5
L	76.1	72.4	68.6	58.8	60.1	61.3	44.9	52.9	60.9

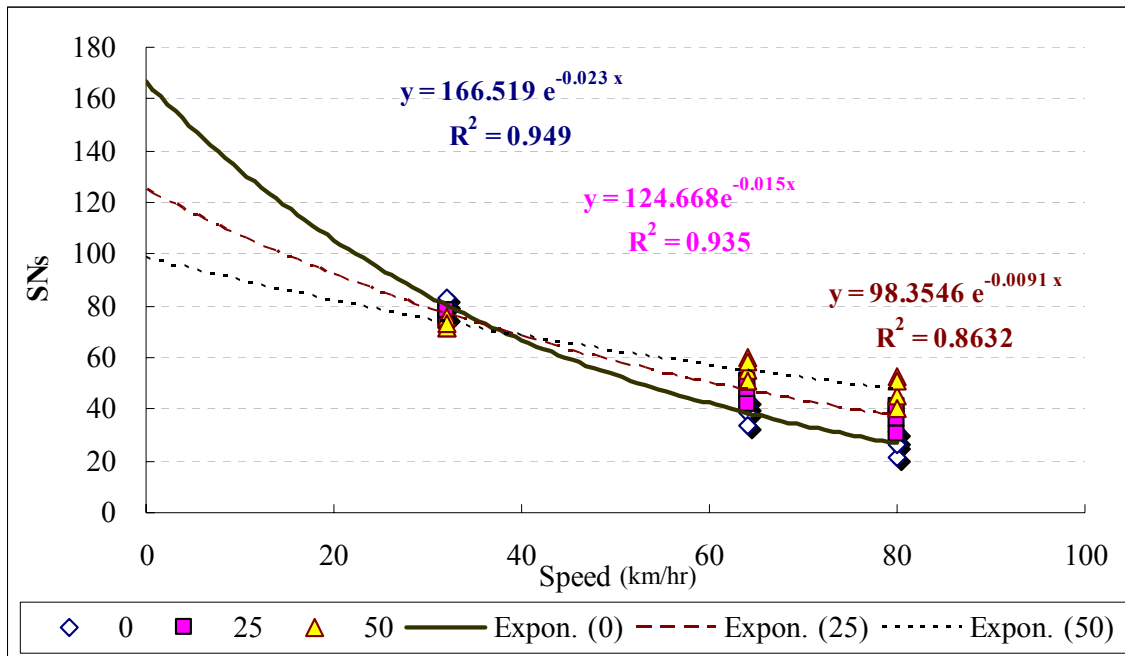


Figure 4.9 SN_S Friction Models for Sections E through H at 0, 25 and 50°C

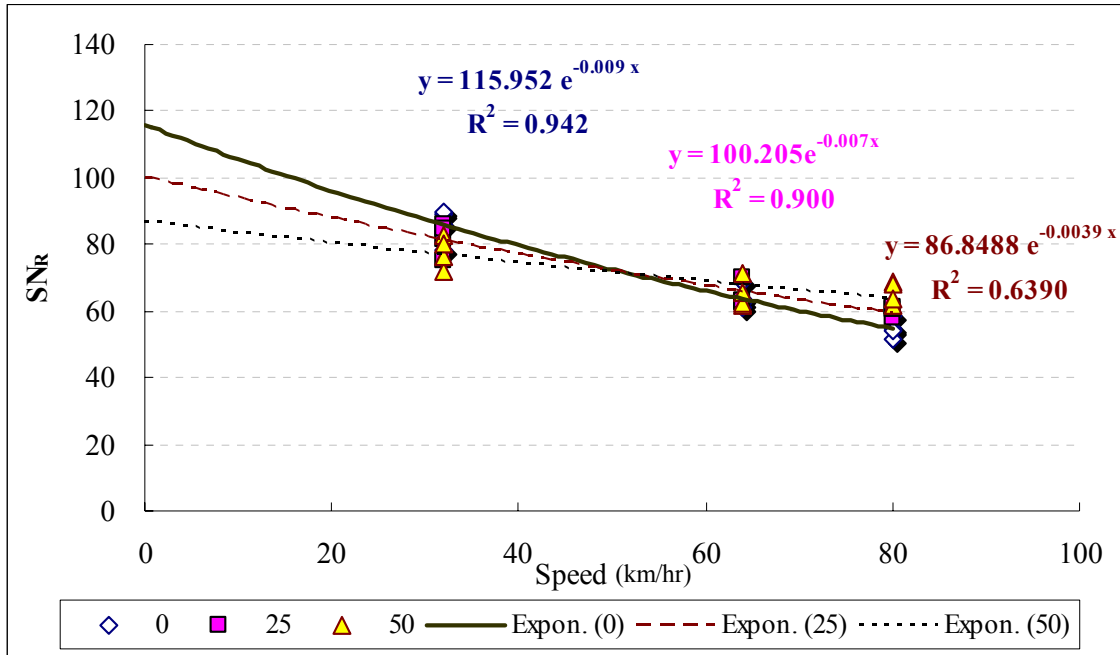


Figure 4.10 SN_R Friction Models for Sections E through H at 0, 25 and 50°C

Both Figures verify the trends previously observed; both the SN₀ and PNG decrease when temperature increases. Furthermore, in the case of the measurements obtained with smooth tire (Figure 4.9) the friction models intersect a speed close to 32 km/hr (20 mph), confirming that there is not significant effect of temperature on the friction measured for the SM-9.5D surface mix. The models for the friction measured with the ribbed tire (Figure 4.10) intercept close to 64 km/hr (40 mph) and are still very close at 80 km/hr; which is also consistent with previous findings.

4.3 Effect of Water on Pavement Temperature

The measurements obtained for the tests conducted to investigate the potential cooling effect of the sprayed water on pavement temperature are presented in Table 4.14. Sites 1, 2, and 3 correspond to a HMA street pavement, a parking lot, and a play ground, respectively.

Table 4.14 Average Surface Temperature (°C) Data of the Temperature Tests

Weather	Date	Time	Site	Surface Temp.		Water Temp.
				Dry	Wet	
Cloudy	10/20/2002	1:45	1 ⁽¹⁾	17.6	17.4	18.8
		2:15		18	17.2	18.8
		2:45		19.2	17.5	18.8
		4:06		18.3	16.6	18.8
		1:45	1 ⁽²⁾	17.4	17.3	16.5
		2:15		18.1	16.8	16.5
		2:45		19.6	17.5	16.5
		4:06		18.6	15.6	16.5
		1:45	2	19.5	19.3	18.4
		2:15		20.5	18.6	18.4
		2:45		21.5	19.3	18.4
		4:06		20.3	17.4	18.4
		1:45	3	18.1	17.4	17.3
		2:15		19.3	17.1	17.3
		2:45		20.5	17.8	17.3
		4:06		18.2	16.2	17.3
Sunny	10/22/2002	5:30	1	24.6	23.7	18.1
		5:52		21.5	23.2	18.5
		7:30		16.2	14.2	17.7
		5:31	2	25.2	24.5	18.1
		5:53		21.7	21.5	18.5
		7:32		15.9	15.1	17.7
		5:33	3	20	17.8	18.1
		5:55		18.8	15.9	18.5

⁽¹⁾ First site 1 testing area; ⁽²⁾ Second site 1 testing area.

The significance of the temperature difference between wet and dry pavements was tested using paired t-test. A 1.5°C difference was considered acceptable and a 0.05 level of significance was used. The results are presented in Table 4.15.

Table 4.15 Paired T-test of Temperature Effect of Water on Pavement

Weather	Cloudy				Sunny			All
Site	1	2	3	All	1	2	All	
Hypothesized Mean Difference	1.5	1.5	1.5	1.5	1.5	1.5	1.5	1.5
Degree of Freedom	7	3	3	15	4	4	11	27
t Statistic	-0.40	0.52	0.94	0.44	-0.82	-2.46	-0.95	-0.40
t Critical one-tail	1.89	2.35	2.35	1.75	2.13	2.13	1.80	1.70
P(T<=t) one-tail	0.35	0.32	0.21	0.33	0.23	0.03	0.18	0.34

The P values for one-tail test indicate that there is no enough statistical evidence that the difference between the paired means is more than the hypothesized 1.5°C. Hence, the overall cooling effect of water on the pavement is not significant and it was appropriate to ignore it in the analysis.

4.4 Summary and Discussion

The results of the statistic analysis show that, for the standard wearing surface mixes, pavement temperature has a significant effect on the pavement frictional properties. In addition, both parameters of the Penn State Model, SN_0 and PNG, tend to decrease with increased pavement temperature. The decrease in SN_0 could be due to less exposed pavement microtexture because the asphalt binder is softer at higher temperatures and may tend to cover more of the aggregate. This would reduce the adhesion component of the tire-pavement friction. Since PNG is also reduced at high temperature, the effect is compensated and reverted at higher speeds because the slope of the skid versus speed curve is flattened. This is shown in Figure 4.11, which depicts the friction-speed models for sections E through H (SM-9.5D) using the smooth and ribbed tires.

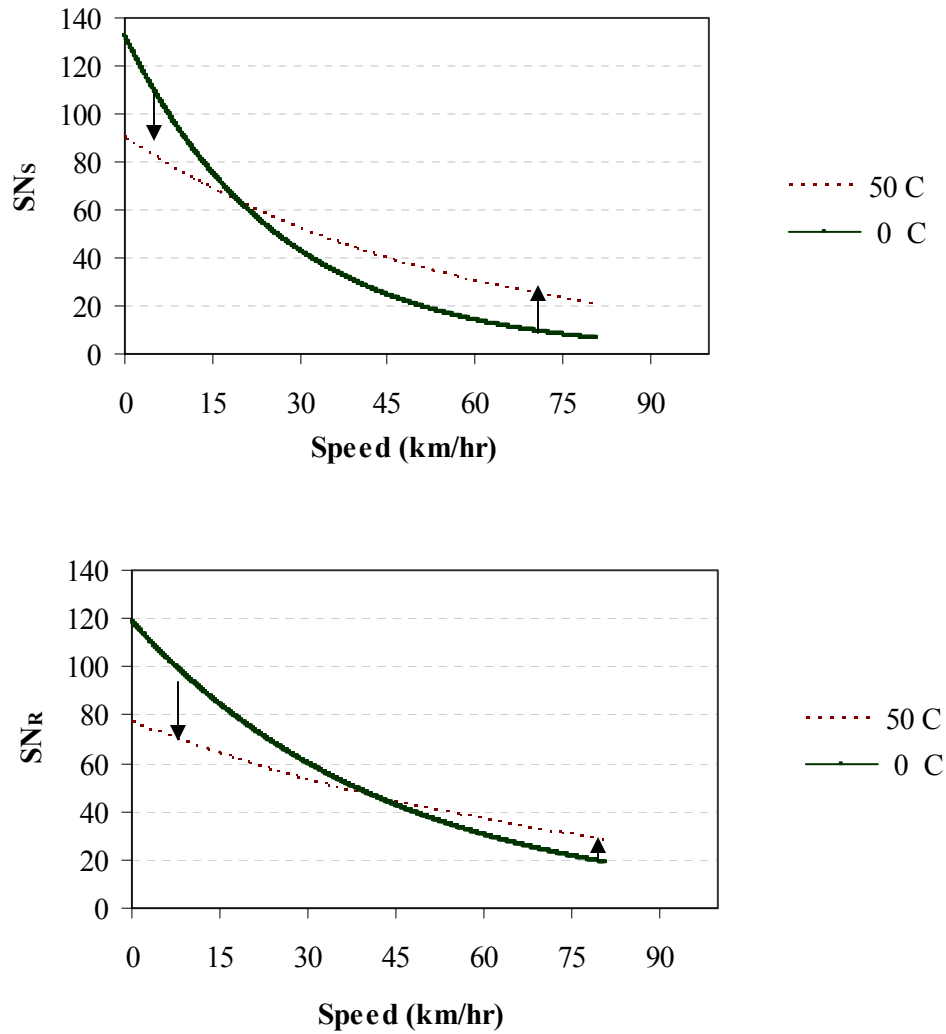


Figure 4.11 Skid Number versus Speed at Different Temperatures

Based on the models obtained, a temperature-dependent model as presented in Equation 4.1 can be developed for each wearing surface HMA mix.

$$SN(T) = (a + bT) * e^{-\left[\frac{(c+dT)}{100}\right] * V} \quad (4.1)$$

where

SN(T) = skid number at certain pavement temperature;

T = pavement temperature;

V = speed (km/hr); and

a, b, b, c = are regression parameters.

The temperature-dependent friction models obtained for the SM-9.5D mix (sections E through H) are presented in Equations 4.2 and 4.3. Similar models could be established for the other mixes.

$$SN_S(T) = (159 - 1.14T) * e^{-\left[\frac{(2.27-0.02T)}{100}\right]*V} \quad (4.2)$$

$$SN_R(T) = (118 - 0.73T) * e^{-\left[\frac{(1.00-0.01T)}{100}\right]*V} \quad (4.3)$$

Where

$SN_S(T)$ = skid number using the smooth tire for SM 9.5D at temperature T;

$SN_R(T)$ = skid numbers using the ribbed tire for SM 9.5D at temperature T;

T = pavement temperature (°C); and

V = testing speed (km/hr).

Chapter 5

Findings and Conclusions

Environmental factors, such as temperature, rainfall, and dry days before the test day, cause seasonal variations in the frictional properties of pavements. Although several researchers have attempted to explain and quantify the effect of temperature on pavement friction, this effect remains to be completely understood. This thesis attempted to quantify the effect of pavement surface temperature on the frictional properties of the pavement-tire interface. To accomplish this, tests conducted on seven different wearing surfaces and under different climatic conditions were analyzed. Due to the short duration of this study and the low traffic on the facility, only short-term effects of temperature on pavement friction were investigated.

5.1 Findings

The analysis produced the following findings relevant to the temperature effect on pavement frictional properties:

- A limited scale complementary test suggested that the water sprayed during testing has no significant cooling effect on the pavement temperature.
- Both parameters of the Penn State Model, SN_0 and PNG, were found to be negatively correlated with pavement temperature; both parameters decrease with increased pavement temperature.
- The linear regression analysis of the individual skid numbers for the three target speeds against temperature showed that different SuperPave HMA exhibited similar patterns. The analysis indicated the following:

- At low speeds, i.e., less than 35 km/hr (22mph) for the smooth tire and 50 km/hr (31mph) for the ribbed tire, pavement friction tends to mildly decrease with increased pavement temperature.
- At higher speeds friction measurements are either insensitive to pavement temperature or tend to slightly increase with increased temperature.
- Similar results were obtained for the friction measurements conducted using the smooth and ribbed tire. However, the measurements using the ribbed tire were less sensitive to temperature.
- Due to the nature of the mix, the friction measurements on the open graded friction course (OGFC) surface are insensitive to temperature changes.

5.2 Conclusions

The main conclusion of this investigation is that pavement temperature has a significant effect on pavement frictional measurements and on the sensitivity of the measurements to the test speed. Both the skid number at zero speed (SN_0) and the percent normalized gradient (PNG) tend to decrease with increased pavement temperature. This results in the pavement temperature effect on the measured skid number being dependent on the testing speed. For the standard wearing surface mixes studied, at low speed pavement friction tends to decrease with increased pavement temperature. At high speed, the effect is reverted and pavement friction tends to increase with increased pavement temperature. Temperature-dependent friction versus speed models were established for one of the mixes studied. These models can be used to define temperature correction factors.

Chapter 6

Recommendations

Although the analysis found a significant effect of pavement temperature on pavement friction and the trend of change at different speeds, further studies are recommended to fully explain the pavement temperature effect on the pavement frictional properties. The main recommendations are listed following.

- Since the pavement temperature may also represent the tire temperature, the trend of changes found in the analysis could be partially attributed to change of tire temperature. Therefore, a future study focusing on the effect of tire temperature on pavement frictional properties is recommended.

- Although a clear trend of change of PNG with temperature was found, the mechanism that causes the PNG decrease with increased temperature is unclear. Further studies are needed to have a correct understanding of this mechanism.

References

- Agrawal S. K. and J. J. Henry (1979) "Technique for Evaluating Hydroplaning Potential of Pavements." Transportation Research Record, No. 633, 1p.
- Al-Qadi, I. L., W. M. Nassar, A. Loulizi, G. W. Flintsch, and T. Freeman (2000) "Flexible Pavement Instrumentation at the Virginia Smart Road." Presented at 79th Transportation Research Board Annual Meeting, Washington, DC, Jan.
- American Society for Testing and Materials (2000) "Calculating International Friction Index of a Pavement Surface." ASTM E-1960, Annual Book of ASTM Standards, Vol. 4.03.
- American Society for Testing and Materials (2000) "ASTM Definitions of Terms Relating to Traveled Surface Characteristics." ASTM E-867, Annual Book of ASTM Standards. Vol. 4.03.
- American Society for Testing and Materials (2000) "Skid Resistance of Pavements Using a Full-Scale Tire." ASTM E-274-97, Annual Book of ASTM Standards. Vol. 4.03.
- American Society for Testing and Materials (2000) "Standard Practice for Calculating International Friction Index of a Pavement Surface." ASTM E-1960-98, Annual Book of ASTM Standards. Vol. 4.03.
- American Society for Testing and Materials (2000) "Standard Rib Tire for Pavement Skid-Resistance Tests." ASTM E-501, Annual Book of ASTM Standards. Vol. 4.03.
- American Society for Testing and Materials (2000) "Standard Smooth Tire for Pavement Skid-Resistance Tests." ASTM E-524, Annual Book of ASTM Standards. Vol. 4.03.
- Anderson D. A., W. E. Meyer, and J. L. Rosenberger (1984) "Development of a Procedure for Correcting Skid-Resistance Measurements to a Standard End-of-Season Value." Transportation Research Record, No. 1084, 40-48p.
- Bowden F. P. and D. Tabor (1950) "The Friction and Lubrication of Solids." Oxford University Press, London.
- Burchett J. L and R. L. Rizenbergs (1980) "Seasonal Variations in the Skid Resistance of Pavements in Kentucky." Transportation Research Record, No. 788, 12p.

- Crouch L. K., J. D. Gothard, G. Head and W.A. Goodwin (1995) "Evaluation of Textural Retention of Pavement Surface Aggregates." Transportation Research Record, No. 1486, 91p.
- Dahir S. H., J. J. Henry and W. E. Meyer (1979) "Final Report: Seasonal Skid Resistance Variations." Pennsylvania Department of Transportation, Harrisburg.
- Dahir S. H., W. E. Meyer and R. R. Hegmon (1976) "Laboratory and Field Investigation of Bituminous Pavement and Aggregate Polishing." Transportation Research Record, No. 584, 1-14p.
- Davis R. M. (2001) "M.S. Thesis: Comparison of Surface Characteristics of Hot-Mix Asphalt Pavement Surfaces at the Virginia Smart Road." Virginia Tech.
- Diefenderfer B. K. (2000) "Ph.D. Dissertation: Moisture Content Determination and Temperature Profile Modeling of Flexible Pavement Structures." Virginia Tech.
- Elkin B. L., K. J. Kercher and S. Gulen (1980) "Seasonal Variation in Skid Resistance of Bituminous Surfaces in Indiana." Transportation Research Record, No. 777, 50-58p.
- FHWA, Nationwide Personal Transportation Survey (1990) "NPTS Databook." FHWA Report FHWA-PL-94-010.
- Gandhi P.M., B. Colucci and S. P. Gandhi (1991) "Polishing of Aggregates and Wet-Weather Accident Rates for Flexible Pavement." Transportation Research Record, No. 1300, 71-79p.
- Giles C.G. and B.E. Sabey (1959) "A Note on the Problem of Seasonal Variation in Skidding Resistance." Virginia Highway Research Council, Charlottesville, VA.
- Goodenow, G. L. (1967) "The Design and Construction of the General Motors Proving Ground Model II Coefficient of Friction Vehicle." Presented to ASTM Committee E-17.
- Henry J. J. (1986) "Tire Wet Pavement Traction Measurement: A State-of-the-Art Review." ASTM STP 1164, 4p.
- Henry J. J. (2000) "Evaluation of Pavement Friction Characteristics, A Synthesis of Highway Practice." NCHRP Synthesis 291, 7p.
- Henry J. J. and J. C. Wambold (1996) "Use of Smooth-Treaded Tire in Evaluating Skid Resistance," Transportation Research Record, No. 1348, 35-41p.

- Hill B. J. and J. J. Henry (1978) "Short Term, Weather-Related Skid Resistance Variation," Transportation Research Record, No. 836, 76-81p.
- Hill B.J. and J. J. Henry (1982) "Surface Materials and Properties Related to Seasonal Variations in Skid Resistance." ASTM STP 763, 5p.
- Hill B.J. and J. J. Henry (1982) "Mechanistic Model for Predicting Seasonal Variations in Skid Resistance." Transportation Research Record, No. 946, 29-37p.
- Hosking J. R. and G. C. Woodford (1976) "Measurement of Skid Resistance Part II, Factors Affecting the Slipperiness of a Road Surface", Transportation Road Research Lab (U.K.), Report LR 346.
- Huang E.Y. and T. Ebrahimzadeh (1973) "Laboratory Investigation of the Effect of the Particle Shape Characteristics and Gradation of Aggregates on the Skid Resistance of Asphalt Surface Mixtures." ASTM STP 530, 117p.
- Jayawickrama P. W. and B. Thomas (1997) "Correction of Field Skid Measurements for Seasonal Variations in Texas." Transportation Research Record, No. 1639, 2p
- Kulakaowski B. T. (1993) "Mathematical Model of Skid Resistance as a Function of Speed." Transportation Research Record, No. 1311, 26-32p.
- Kummer H. W. and W. E. Meyer (1962) "Measurement of Skid Resistance, Symposium on Skid Resistance." ASTM Special Technical Publication, No. 326, 3-28p.
- Leu, M. C. and J. J. Henry (1976) "Prediction of Skid Resistance as a Function of Speed from Pavement Texture." Transportation Research Record, No.946, TRB, National Research Council.
- Meyer W. E. (1968) "Friction and Slipperiness." Highway Research Record No. 214, 13-17p.
- Mitchell, J.C., M.I. Phillips, and G. N. Shah (1986) "Report No. FHWA/MD-86/02: Seasonal Variation of Friction Numbers." Maryland Department of Transportation (MDOT), Baltimore.
- National Climatic Data Center (1998) "Climate of 1998 Annual Review: Month-by-Month Variability in U.S." Asheville, NC.
- National Transportation Safety Board (1980) "Special Study: Fatal Highway Accidents on Wet Pavement." Washington, D. C.

- Oliver, J.W.H. (1989) "Seasonal Variation of Skid Resistance in Australia." Australia Road Research Board, Special Report No. 37.
- PIARC (1995) "PIARC Report 01.04T: International PIARC Experiment to Compare and Harmonize Texture and Skid Measurements." The World Road Association, Paris.
- Roberts F. L., P. S. Kandhal, E. R. Brown, D.Y. Lee and Thomas W. Kennedy (1996) of "HMA Materials, Mixture Design, and Construction." 2nd Edition, NAPA Research and Education Foundation.
- Runkle S. N. and D. C. Mahone (1980) "Variation in Skid Resistance over Time." Virginia Highway & Transportation Research Council, 10-13p.
- Smith R.N. and L.E. Elliott (1975) "Evaluation of Minor Improvements: Grooved Pavement." Supplemental Report, CA-DOT-TR-2152-11-75-01, Office of Traffic, California Department of Transportation.
- Smith B. J. and R.G. Pollock (1997) "Textural and Mineralogical Characterization of Kansas Limestone Aggregates in Relation to Physical Test Results." FHWA-KS-97/4, Final Report, 91p.
- Tabor D. (1958) "The Importance of Hysteresis Losses in the Friction of Lubricated Rubber." Virginia Highway Research Council, Proc First INTL SKID PREV CONF, PART 1, 211-218p.
- Takino, H., et al. (1998) "Effect of Cohesion Loss Factor on Wet Skid Resistance of Tread Rubber." Tire Science and Technology, TSTCA, Vol. 26, No. 4, 258-276p.
- Tung J. S. N., J. J. Henry and S. H. Dahir (1977) "Statistical Analysis of Seasonal Variations in Pavement Skid Resistance." The Pennsylvania Transportation Institute, Department of Transportation Bureau of Materials, Testing and Research, Research Report No. 75-10.
- Virginia Department of Transportation (VDOT) (2002) "Road and Bridge Specifications 2002." Richmond, Virginia.
- Wambold J. C., J. J. Henry, and R. R. Hegmon (1986) "Skid Resistance of Wet-Weather Accident Sites." ASTM STP929, 47-60p.
- Whitehurst E. A. and J. B. Neuhardt (1986) "The Tire Pavement Interface: Time History Performance of Reference Surfaces." ASTM STP 929, 61-71p.

Appendix A: Raw Skid Test Data

Appendix B: Pavement Surface Temperature Data

VITA

Yingjian Luo was born on February 28, 1974 in the Sichuan Province of China to Wenquan Luo and Bangrong Deng. He graduated from No. 2 High School of Yibin County, Sichuan, China in July 1993. In July 1997, the author graduated from Chongqing Jiaotong University in Chongqing, China and went to the Philippines to work on a world-bank financed project, the Kabankanan to Basay Coastal Highway Restoration Project. He then worked on Guiyang to Xinzhai National Highway Project in China. In August 2001, the author began his study in the Civil Engineering Department at Virginia Polytechnic Institute and State University. He worked as a graduate research assistant and expects his master's degree in January 2003.